

CONTENTS

ABSTRACT.....	II
DEDICATIONS.....	III
CONTENT.....	IV
LIST OF FIGURES.....	VI
LIST OF TABLES.....	VIII
1 BACKGROUND OF STUDY	1
1.1 INTRODUCTION	1
1.2 IMPORTANCE OF STUDY	2
1.3 THESIS OBJECTIVES	2
1.4 SCOPE AND LIMITATIONS OF STUDY	2
1.5 THESIS LAYOUT.....	3
2 GROUND PENETRATING RADAR.....	4
2.1 RADAR.....	4
2.2 GROUND PENETRATING RADAR (GPR).....	5
2.3 BASIC PRINCIPLE OF GPR	5
2.4 WHY GPR.....	10
Lastly, Comparing GPR to other geophysical surveying methods, GPR provides the broadest range of geological feature detection; including glaciers, sediment thickness, bedrock, fractures, faults, groundwater, voids and sinkholes.....	11
2.5 APPLICATIONS OF GPR.....	11
2.5.1 <i>Archaeology</i>	11
2.5.1.1 Concordia Temple in Agrigento, Sicily	11
2.5.1.2 Structural Control of Historic Buildings	12
2.5.2 <i>Environmental</i>	15
2.5.2.1 Mining	Error! Bookmark not defined.
2.5.2.2 Quarry.....	15
2.5.2.3 Unconventional Deep-water Investigation of Drilling Obstructions.....	16
2.5.3 <i>Engineering</i>	17
2.5.4 <i>Forensic uses</i>	18
2.5.4.1 Location of Human Burials.....	18
2.6 GPR INSTRUMENTATION	19
2.7 STATE OF THE ART OF GPR	20
2.7.1 <i>Introduction</i>	20
2.7.2 <i>How modern is Noggin and PulseEKKO?</i>	20
2.7.3 <i>Noggin and PulseEKKO Software</i>	22
2.7.4 <i>Improvement in GSSI</i>	23
2.7.4.1 The Past, Present and Future of GPR Antennas	23
2.7.5 <i>MALÅ GPR</i>	34
3 SOIL CONTAMINATION	39
3.1 INTRODUCTION	39
3.2 CHARACTERISATION OF SITE (SOIL).....	39
3.3 TYPES OF SOIL CONTAMINANTS.....	41
3.3.1 <i>Light Non Aqueous Phase Liquid (LNAPL)</i>	42
3.3.1.1 Introduction.....	42
3.3.1.2 LNAPL Transport through porous media	44

3.3.1.3	Contaminant Phase Distribution	44
3.3.1.4	LNAPL transport parameters	45
3.3.1.4.1	NAPL migration at the pore scale	45
3.3.1.4.1.1	Density	45
3.3.1.4.1.2	Viscosity	46
3.3.1.4.1.3	Interfacial tension	46
3.3.1.4.1.4	Wettability	46
3.3.1.4.1.5	Capillary pressure	47
3.3.1.4.2	NAPL migration at the field scale	47
3.3.1.4.2.1	Fluid and porous media properties	47
3.3.1.4.2.2	Nature of LNAPL released	48
3.3.1.4.2.3	Subsurface heterogeneity	49
4	GPR FOR SOIL CONTAMINATION	50
4.1	INTRODUCTION	50
4.2	DIELECTRIC PROPERTIES OF GEOLOGICAL MATERIALS	50
4.3	DETECTING CONTAMINANTS WITH RADAR DATA	52
4.4	UNDETECTABLE ORGANICS	53
4.5	LNAPL DETECTION AND MAPPING WITH GPR	54
5	CASE STUDIES OF CONTAMINANT DETECTION WITH GPR	57
5.1	CANADIAN FORCE BASE BORDEN	57
5.2	NAVAL AIR STATION	58
5.3	BRAZIL	59
5.4	FT-2-PLUME AT THE WURTSMITH AIR FORCE BASE	59
6	CONCLUSIONS AND RECOMMENDATIONS	61
	REFERENCES	62

LIST OF FIGURES

FIGURE	PAGE
FIGURE 2.1: GPR COMPLETE SYSTEM.....	6
FIGURE 2.2: SIMPLIFIED ILLUSTRATION OF THE OPERATION OF GSSI SIR-3 RADAR UNIT USING THE 300MHZ ANTENNA.....	6
FIGURE 2.3: GPR DATA SHOWING REFLECTION FROM UNDERGROUND STORAGE TANK (WWW.EARTHDYN.COM) ...	7
FIGURE 2.4: 1000MHZ DEEP PENETRATION CONCRETE ANTENNA ON THE LEFT AND COMMERCIAL GPR SYSTEM WITH 25MHZ ANTENNAS ON THE RIGHT.	9
FIGURE 2.5 CONCORDIA TEMPLE IN AGRIGENTO, SICILY.....	11
FIGURE 2.6 SCHEMATIC MAP SHOWING THE LOCATION OF THE 261M OF GPR DATA COLLECTED RELATIVE TO THE VISIBLE STRUCTURE OF THE CONCORDIA TEMPLE ON THE LEFT AND ON THE RIGHT IS (A) SCHEMATIC RECONSTRUCTION OF THE PLAN OF THE TEMPLE, (B) THE NORTHERN LONGITUDINAL SECTION AND (C) THE SOUTHERN LONGITUDINAL SECTION, BASED ON THE ACQUIRED GPR DATA.	12
FIGURE 2.7 THE ARCHAEOLOGICAL SITE OF PORTICUS OCTAVIAE (LEFT) AND THE POOR STATE OF CONSERVATION OF MARBLE OF THE PORTICUS OCTAVIAE (RIGHT)	13
FIGURE 2. 8 A GENERAL VIEW OF THE ZUCCARI PALACE	13
FIGURE 2.9: GPR SECTION CONDUCTED USING THE 500 MHZ ANTENNAS ALONG A 14 M LONG LINE ACROSS THE ARCHITRAVE OF THE PORTICUS OCTAVIAE. NO PROCESSING HAS BEEN APPLIED TO THIS DATA. THIS SECTION CLEARLY SHOWS THE AREAS OF INNER LESIONS (BLACK ARROWS) AND THE FILLED FRACTURES THAT PENETRATE THROUGH THE ENTIRE ARCHITRAVE (WHITE ARROWS).	14
FIGURE 2.10 RADARGRAMS SHOWING THE INTERNAL GEOMETRY OF THE VAULTED CEILING IN THE ZUCCARI PALACE.	14
FIGURE 2. 11 URANIUM EXPLORATION IN AFRICA ON LEFT AND KIMBERLITE EXPLORATION IN TANZANIA ON THE RIGHT.....	15
FIGURE 2.12 BUILDING/DIMENSION STONE INTEGRITY	16
FIGURE 2.13 : A LOCK AT THE WALTER F. GEORGE DAM.	16
FIGURE 2.14 PROCESSED GPR RECORD FOR DATA COLLECTED.....	17
FIGURE 2. 15: GPR IMAGE SHOWING REBAR SPACING AND THICKNESS	17
FIGURE 2.16: VOID IN CONCRETE ON THE LEFT AND GPR IMAGE OF VOID IN CONCRETE ON THE LEFT.....	18
FIGURE 2.17: GPR IN USE ON AN HISTORIC CEMETERY (LEFT) AND A TIME-SLICED GPR MAP OF A 19TH CENTURY CEMETERY SHOWING CORRELATION BETWEEN GEOPHYSICAL ANOMALIES AND EXISTING GRAVE MARKERS (SHOWN IN YELLOW) (RIGHT).....	19
FIGURE 2.18 AN OPERATION MAKING ACQUISITION WITH A SMARTCART GPR.....	21
FIGURE 2. 19: SMARTHANDLE GPR BEING USED BY A MILITARY FOR DATA ACQUISITION.	21
FIGURE 2. 20: SMARTTOW IN OPERATION.	22
FIGURE 2. 21: ROCK NOGGIN GPR BEING USED ON HARD ROCK AND INSIDE A TUNNEL.....	22
FIGURE 2. 22: THE PROFILER IN USE.	24
FIGURE 2. 23: GSSI SIR-20 INSPECTING A BRIDGE DECK.	25
FIGURE 2. 24: SIR-30	26
FIGURE 2. 25: SIR-300 BEING USED TO INSPECT A TUNNEL.	27
FIGURE 2. 26: STRUCTURESCAN MINI.	28
FIGURE 2. 27: RADARGRAM PRODUCED BY THE STRUCTURESCAN MINI VIEWER.....	29
FIGURE 2. 28: RADARGRAM PRODUCED WITH RADAN SOFTWARE.	30
FIGURE 2. 29: STRUCTURESCAN OPTICAL IN OPERATION.....	30
FIGURE 2. 30: STRUCTURESCAN STANDARD INSPECTING CONCRETE WALL.	32
FIGURE 2. 31: SINGLE (LEFT) AND MULTIPLE (RIGHT) MOUNT ANTENNAS ROADSCAN INSPECTING ROAD.....	32
FIGURE 2. 32: BRIDGESCAN GPR ASSESSING BRIDGE DECK, REINFORCED CONCRETE (LEFT) AND ROAD STRUCTURE (RIGHT).	33
FIGURE 2. 33: UTILITYSCAN LOCATING AND MAPPING UNDERGROUND UTILITIES.	34
FIGURE 2. 34: MALA MIRA GPR.	35

FIGURE 2. 35: MALÁ X3M IN OPERATION ON ROUGH TERRAIN AND ON GRASS.....	36
FIGURE 2. 36: MALA ProEx GPR SYSTEM IN USE TO INVESTIGATE THE SUBSURFACE.	37
FIGURE 2. 37: MALA EASY LOCATOR INVESTIGATING THE SUBSURFACE.	38
FIGURE 3. 1: PETROLEUM CONTAMINATED SITE (WWW.TEST-LLC.COM).....	41
FIGURE 3. 2: AMMONIA NITRATE CONTAMINATED SITE (WWW.HYDE-ENV.COM).....	42
FIGURE 3. 3: REPRESENTATION OF LNAPL MOVEMENT IN THE SUBSURFACE (MODIFIED FROM PINDER AND ABRIOLA 1986).....	44
FIGURE 3. 4: CONCEPTUAL LNAPL DISTRIBUTION AFTER LATERAL MIGRATION	45
FIGURE 3. 5: CONTACT ANGLE FOR WETTING AND NON-WETTING FLUIDS. THIS DIAGRAM SHOWS THE WETTABILITY CONFIGURATIONS FOR WATER AND LNAPL (MODIFIED FROM MERCER AND COHEN 1990) ..	46

LIST OF TABLES

TABLE	PAGE
TABLE 2.1: RDP'S OF COMMON GEOLOGICAL MATERIAL (WITH 100 MHZ ANTENNA).....	8
TABLE 2. 2: GPR CENTRAL FREQUENCY, DEPTH OF PENETRATION AND APPLICATIONS.....	23
TABLE 3.1: REPRESENTATIVE PROPERTIES OF SELECTED LNAPL CHEMICALS COMMONLY FOUND AT SUPERFUND SITES.....	20
TABLE 3.2: COMMON PETROLEUM PRODUCTS OF SELECTED LNAPL.....	21
TABLE 4.1: EXPERIMENTAL INVESTIGATIONS OF DIELECTRIC PROPERTIES OF GEOLOGICAL MATERIALS.....	30
TABLE 4.2: TOP 10 ORGANIC CHEMICAL CONTAMINANTS	31

1 BACKGROUND OF STUDY

1.1 Introduction

Ground penetrating radar is a simple geophysical technique that can collect and record information of the subsurface. It is a near surface method that provides high resolution three-dimensional images of the subsurface of the earth. Ground penetrating radar can also be considered as a non – invasive geophysical method that can be used to extract the geometrical and physical properties of targets buried beneath the subsurface.

This geophysical technique has been in existence for quite a long time now. Its first application was reported in 1929 where it was used to delineate the depth of ice in Austria and ever since, it has been applied to a wide range of fields including groundwater resources, mineral exploration, archaeological studies, etc. One field where this technique is mostly used is in the field of environmental geophysics where it is applied to locate and predict the fate and transport of contaminants in the subsurface.

The contaminants are either solid or liquid hazardous substances mixed with the naturally occurring soil. Contaminants in the soil are usually physically or chemically attached to soil particles, or, if they are not attached, are trapped in the small spaces between soil particles. The contaminations typically arise from the rupture of underground storage tank, application of pesticides, and percolation of contaminated surface water to subsurface strata, oil and fuel dumping, leaching of wastes from landfills or direct discharge of industrial wastes to the soil. The most common chemicals involved are petroleum hydrocarbons, solvents, pesticides, lead and other heavy metals. The occurrence of this phenomenon is in correlation with the degree of industrialization and intensities of chemical usage.

Organic contaminants such as Light Non – Aqueous Phase Liquids (LNAPLs) present a serious threat to groundwater, land and public health throughout the developed and developing world. Most LNAPLs are both sparingly soluble and highly mobile and therefore assessing their time – varying concentrations and sub – surface distribution could be very difficult particularly in complex, near – surface industrial environments. We are very much concerned about soil contamination because of the great danger it poses to human health, ecosystems, groundwater, etc. everywhere.

The traditional way of site investigation and characterization of contaminants includes excavation, drilling, sampling and need for a distribution modeling. These are necessary in the determination of the exact nature of any contamination event. These processes are most of the time expensive, destructive and require a long time to accomplish. With regards to the sampling, only a limited volume of the subsurface can be sampled, there is always the risk of contacting or further spreading the contaminant and there could be problems with the labelling.

Moreover, in recent times and as a result of the numerous pitfalls with regards to the traditional methods of site investigation and characterization of contaminants, non-destructive geophysical investigation techniques such as electrical resistivity, induced polarisation, electromagnetic conductivity and, more particularly, Ground Penetrating Radar have become increasingly popular.

Ground penetrating radar has inconceivable appeal as a non – invasive means of imaging the subsurface thereby making it environmentally friendly. There is also the availability of borehole radar systems that allows the sampling of the subsurface using new or existing boreholes but this type of radar will not be considered with regards to this thesis.

1.2 Importance of study

The GPR technique has numerous advantages as compared to the traditional methods of contaminant mapping. Some of these advantages are further illustrated in the second chapter of this thesis. The outputs or findings of this project, through the analysis of the results, I believe, will also contribute enormously to this field of study.

Contaminant plumes, either LNAPLs or DNAPLs usually pose a great danger to life in various ways either directly or indirectly because of their hydrocarbon content. The chemicals they contain make the contamination to be electrically conductive and the GPR technique depends on the conductivity of the subsurface materials. This makes the GPR technique of great relevance in mapping the contaminants.

Many contaminant plumes such as the LNAPLs are sparingly soluble and highly mobile. This mobility leads to their various distributions in the subsurface. Through the studying of their distributions and mobility, the future locations of the contaminants could be predicted. This is another reason why this thesis is of great importance.

1.3 Thesis objectives

The main objectives of the research project are:

- To use ground penetrating radar in detecting the present location of contaminants.
- To map contaminants.

1.4 Scope and Limitations of study

This thesis describes the application of ground penetrating radar technique in the detection and mapping of subsurface contaminant plumes. Our main focus is on dealing with Light Non-Aqueous Phase Liquids (LNAPLs). This thesis is not concerned with dealing Dense Non-Aqueous Phase Liquids (DNAPLs) but their detection and mapping will be an added advantage.

The ground penetrating radar has a depth range in which it operates. This research discusses the detection and mapping within the GPR's operation depth. We will not go beyond the depth of operation of the instrument.

1.5 Thesis layout

This thesis is organized in various chapters. Chapter one is an introductory to the thesis. This chapter gives a general overview of what this thesis is about. It presents background knowledge about ground penetrating radar and contaminants, the thesis objectives, the problems to be investigated and the limitations of our study.

Chapter two properly discusses the ground penetrating radar. It commences by giving a little insight about what radar is, a brief history of radar and some uses of radar. It further goes on to describe the ground penetrating radar, its operating principles, some merits, applications, instrumentation, the current improvements and the future.

Chapter three talks about the soil contamination. It involves a discussion of the various types of contamination and their effects. There is also a section for site characterization where discussions are made about the Laws concerning studies and methodologies for contaminated sites characterization. Here, we get information about the two contaminants threshold concentration levels.

The next chapter which is chapter four discusses the ground penetration radar and soil contamination. It gives information about how GPR can be applied in the detection of contaminants. New improvements in the GPR technique are also talked about in this chapter.

Chapter five describes case histories of how GPR was used to detect contaminants. Different scenarios where the ground penetrating radar was used to detect and map contaminant plumes are discussed here.

Chapter seven is the last chapter of this thesis. The understanding gained in this project is used to draw conclusions and make some recommendations for future purposes.

2 Ground Penetrating Radar

2.1 Radar

Radar is an object-detection system by using radio waves which is a part of the electromagnetic spectrum to determine the range, altitude, direction, or speed of both moving and fixed objects such as aircraft, ships, spacecraft, guided missiles, motor vehicles, weather formations, and terrain. The radar antenna transmits pulses of radio waves which bounce off any object in their path. The object returns a tiny part of the wave's energy to a dish or antenna which is usually located at the same site as the transmitter.

The history of RADAR began in 1886 with a German Physicist by name Heinrich Hertz when he demonstrated that electromagnetic waves can be reflected off solid objects. In 1895 **Alexander Popov**, a physics instructor at the Imperial Russian Navy School in Kronstadt (Russian town), developed an apparatus using a tube that could detect distant lightning strikes. Christian Hulsmeyer, a German researcher, was the first to use radio waves to detect “the presence of distant metallic objects” (<http://www.innovateus.net/science/what-are-different-uses-radar>).

The term RADAR is an acronym which was coined in mid 1930's by British and American scientists who conducted experiments with devices to locate objects such as ships and aircrafts by the reflection of radio waves. The process was originally called Radio Location, but as subsequent experiments proved to be successful a well structured name was chosen; '**RA**dio **D**etection **A**nd **R**anging'. Hence, the name RADAR (www.airwaysmuseum.com).

A radar system usually operates in the ultra-high-frequency (UHF) or the microwave part of the radio-frequency (RF) spectrum. Radar is something that is in use all around us, although it is normally invisible. It has diverse applications in numerous fields including traffic control, radar astronomy, military applications, flight control systems, meteorology, outer space surveillance, marine applications, geology, geophysics, etc.

Police use radar to detect the speed of passing motorists. Air traffic control uses radar to track planes both on the ground and in the air, and also to guide planes in for smooth landings. In Radar astronomy, radar is used to observe nearby astronomical objects by reflecting microwaves off target objects and analyzing the echoes. The military uses it to detect the enemy and to guide weapons in locating their targets. Meteorologists use radar to track storms hurricanes and tornadoes and also important tool in weather forecasting and helps make the forecasts more accurate. NASA uses radar to map the Earth and other planets, to track satellites and space debris and to help with things like docking and maneuvering. In marine applications, radars are used to measure the bearing and distance of ships to prevent collision with other ships, to navigate and fix their positions at sea when within range of shore or other fixed references such as islands, buoys and light ships. The automatic opening of the doors when one enters a supermarket is also common application of radar in everyday life.

The first ground penetrating radar survey was performed in Austria in 1929 to sound the depth of a glacier (Stern, 1929, 1930). In the latter part of the 1950's, the United States Air force radars were able to detect the depth of ice as their planes tried to land in Greenland. This prompted further investigation into the use of radar to map subsurface, subsoil properties and the water table. Radar was also used for space missions to the moon in 1967. Before the

early 1970's, anyone who wanted to do GPR had to build his/her own. It was in 1972 that Rex Moray and Art Drake started Geophysical Survey Systems Inc. so as to sell GPR systems commercially and ever since that time, there has been a sudden increase in the research and publications and as well as applications which were mainly promoted by the Geological Survey of Canada, the United States Army Cold Regions and Engineering Laboratory (CRREL) and other institutions. Presently, there are many companies producing GPR equipments commercially, a lot of companies offering it as a service, several institutions researching into GPR and over 300 patents registered with the Patent Office which are in a way related to the original GPR invention (Olhoeft).

2.2 Ground Penetrating Radar (GPR)

Ground penetrating radar (GPR) as a geophysical technique is a high frequency electromagnetic method that uses radio pulses to image the subsurface. The frequencies used are the Ultra High Frequencies (UHF) or the Very High Frequencies (VHF) of the microwave band of the radio spectrum. Precisely, GPR works within the range from 10MHz to 2GHz (<http://www.geo-radar.pl/en/methods/georadar/working/>). It is a non – destructive and non – invasive method that can use electromagnetic wave propagation and scattering to image, locate and quantitatively identify changes in electrical and magnetic properties in the subsurface.

2.3 Basic Principle of GPR

A GPR system comprises a signal generator, a transmitting antenna, a receiving antenna and a receiver that may or may not have recording facilities. Other advanced systems have an onboard computer to aid in the processing of data both during the data acquisition on the field and post- recording. A GPR system radiates pulses of high-frequency electromagnetic energy which propagate away in a broad beam into the ground from a transmitting antenna. The generated high frequency pulses of radio waves are a characteristic of or depend on the antenna being used for the survey. The receiving antenna is also set to scan at a fixed rate and it is normally up to 32 scans per second. The number of scans depends on the type of system being used. Radio waves usually travel at high velocities. The total travel time, which is the travel time from transmission of the signal to the time of reception at the receiving antenna ranges from a few tens of nanoseconds to several thousand nanoseconds. Each of the scanning lasts the range of the two-way travel time and it can be set from a few tens to several thousand nanoseconds.



Figure 2.1: GPR complete system

The electromagnetic wave propagates into the ground at a speed which is related to the electrical properties of the materials present in the subsurface. When the electromagnetic wave encounters the interface of two materials where there is a change in the electrical conductivity between two materials, a portion of the energy is reflected back to the surface, where it is detected by the receiving antenna and a portion is transmitted downward to deeper material. The reflected signal is amplified, transformed into audio-frequency range and recorded. It is further transmitted to a control unit for processing and display. The greater the contrast between the materials, the greater the amount of radio wave energy reflected. The GPR image, an example of which is shown in Figure 1, is produced from a compilation of the station recordings.

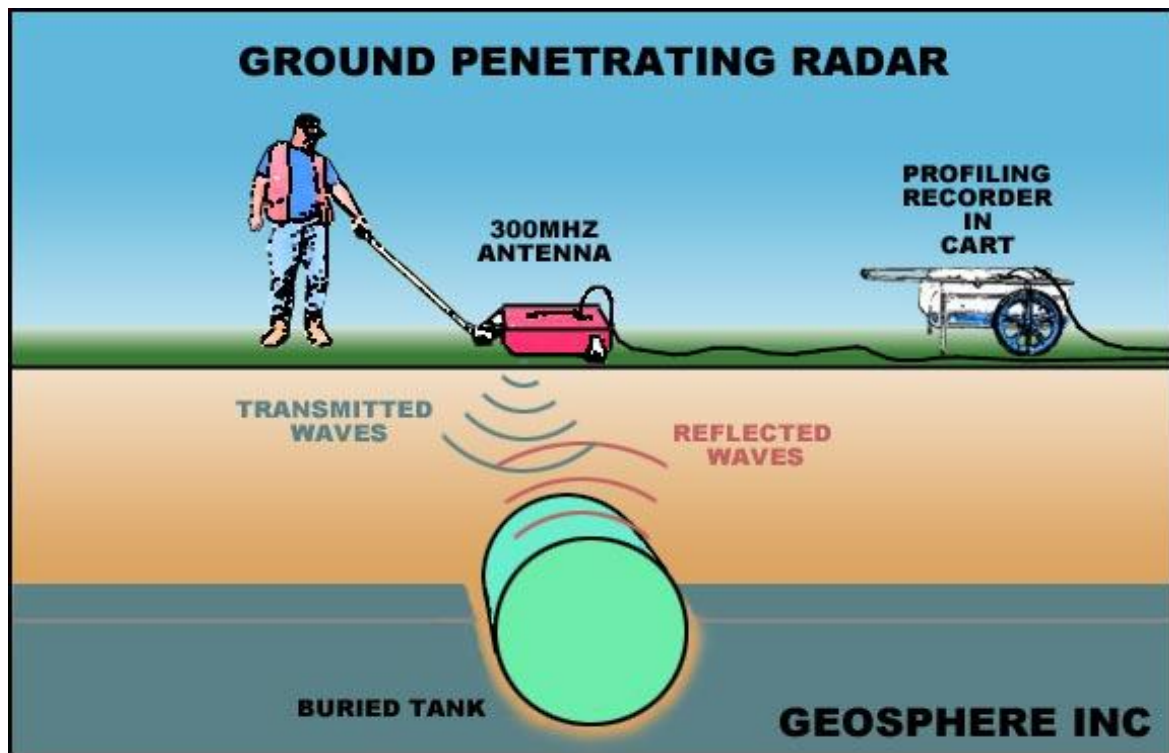


Figure 2.2: Simplified illustration of the operation of GSSI SIR-3 radar unit using the 300MHz antenna

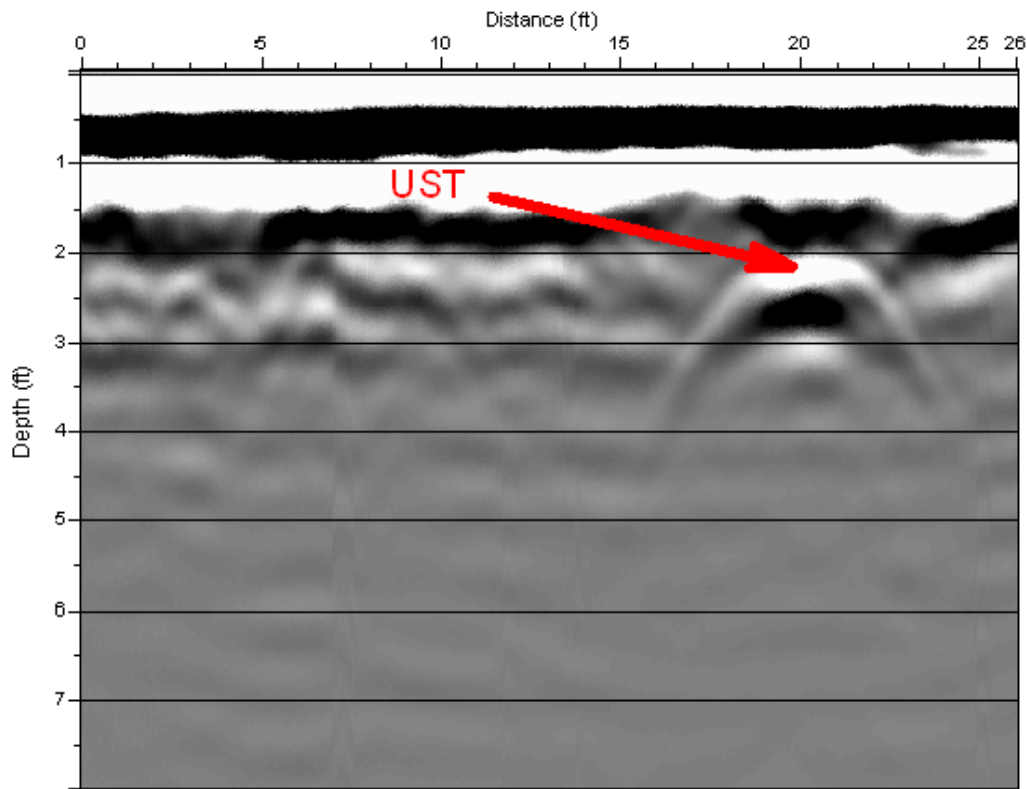


Figure 2.3: GPR data showing reflection from underground storage tank (www.earthdyn.com)

The depth to a reflector (d , in meters) can be determined from the two – way travel time (t , in nanoseconds) and the electromagnetic wave velocity (V , in meters per nanosecond):

$$d = t \times \frac{V}{2}$$

The velocity (V) of the electromagnetic wave can be determined by:

$$V = \frac{c}{\sqrt{\epsilon}}$$

Where ‘ c ’ is the velocity of light in free space equal to 0.2998 meter per nanosecond and ‘ ϵ ’ is the relative dielectric permittivity (RDP). The relative dielectric permittivity, a dimensionless ratio, is the standard unit used to measure radar propagation. It is defined as a measure of a materials capacity to store a charge when an electric field is applied to it relative to the same capacity in a vacuum (Sheriff, 1984). The lower the relative dielectric permittivity of a material, the higher the radar velocity will be of the wave passing through the material. Table 2.1 shows the typical relative dielectric permittivities of several common geological materials.

Table 2.1: RDP's of Common Geological Material (with 100 MHz Antenna)

Material	Relative Dielectric Permittivity	Material	Relative Dielectric Permittivity
Air	1	Dry silt	3 – 30
Fresh water	80	Saturated silt	10 – 40
Ice	3 – 4	Clay	5 – 40
Sea water	81 – 88	Permafrost	4 – 5
Dry sand	3 – 5	Average Surface Soil	12
Saturated sand	20 – 30	Dry Sandy Coastal Land	10
Volcanic Ash/Pumice	4 – 7	Forested Land	12
Limestone	4 – 8	Rich Agricultural Land	15
Shale	5 – 15	Concrete	6
Granite	5 – 15	Asphalt	3 – 5
Coal	4 – 5		

(Conyers and Goodman, 1997)

In addition to, the electromagnetic wave velocity is equal to the product of the wavelength (λ , in meters or feet) and the frequency (f, in cycles per second):

$$V = \lambda f$$

The greater the difference between the relative dielectric permittivity of the material, the larger the amplitude of the generated reflection. Therefore, the reflection generated at the boundaries of two materials can be expressed by the following equation:

$$R = (\sqrt{\epsilon_1} - \sqrt{\epsilon_2}) / (\sqrt{\epsilon_1} + \sqrt{\epsilon_2})$$

R = Coefficient of reflectivity at a Buried Surface

ϵ_1 = Relative Dielectric Permittivity of the Overlying Material

ϵ_2 = Relative Dielectric Permittivity of the Underlying Material

For the production of a good reflection, the difference in dielectric permittivities of the two materials must occur over a short distance. In fact, if RDPs change progressively over a long distance, small changes in reflectivity will occur and very weak reflections will be generated. For instance, if a metallic drum is buried in the ground and the propagation waves strike it, the waves will be reflected 100% and will shadow anything that is directly beneath it.

The antennae can be used in two different ways; Monostatic mode or Bistatic mode. In the monostatic mode the same antenna is used as the transmitting and the receiving antenna whiles in the bistatic mode, two antennae are used with one serving as the transmitting antenna and the other as the receiving antenna.

The changes in conductivity and in dielectric properties could be attributed to the natural hydrogeologic conditions such as bedding, cementation, moisture, clay content, voids and

fractures. Oftently, large changes in dielectric properties exist between geologic materials and man-made structures such as buried utilities or tanks.

How deep the GPR can penetrate into the ground is determined by the electrical conductivity of the ground, and the transmitting frequency. The lower the conductivity, the deeper the penetration of the GPR signal. This is because, as conductivity increases, the electromagnetic energy is more rapidly converted into heat and thereby causing a loss in signal strength at depth. On the other hand, higher frequency signals do not penetrate as far as lower frequencies but higher frequencies normally give a better resolution than the lower frequencies. Therefore, to achieve maximum radar penetration a medium should have low electrical conductivity and high dielectric (or low magnetic permeability). In addition to, the length of the antenna is inversely proportional to the frequency of the GPR. This means that, the longer the length of the antenna, the lower it's frequency and vice versa. For example, a 1000 MHz antenna is about 15 centimeters and can be moved around easily in almost any space, while a 10 MHz antenna is 15 meters long and needs a much larger space in order to operate.



Figure 2.4: 1000MHz Deep Penetration Concrete Antenna on the left and Commercial GPR system with 25MHz Antennas on the right.

Furthermore, the speed of radio waves in any medium depends on the speed of light in free space, the relative dielectric constant and the relative magnetic permeability. The magnetic permeability of a medium is defined as the ability of a medium to become magnetized when an electromagnetic field is imposed upon it (Conyers and Goodman,1997). Also, the success of the GPR technique relies on the medium's variability to allow the transmission of radio waves. Dry sandy soils, rocks and massive dry materials such as granite, limestone and concrete are dielectric or have low magnetic permeabilities. This means that they will allow the passage of most electromagnetic energy without dissipating it. On the contrary, iron-rich materials or materials that contain magnetite, have high magnetic permeabilities (or low dielectric) therefore transmitting radar energy poorly. The more dielectric a material is the less electrically conductive it is.

In addition to, there is a reduction in the signal strength as the radio waves propagate through the ground. First of all, these energy losses occur as a result of reflection or transmission losses that arise at the interface when radio waves propagate through a boundary. Secondly, the reduction in signal strength is also due to a phenomenon known as Mie Scattering. This is

the random scattering of energy due to the presence of objects in the sub-surface with the same order of dimensions as the wavelength of the radar signal. Thirdly, there is loss of energy by the Geometrical spreading of the energy in the sub – surface.

2.4 Why GPR

The conventional approach used in the investigation of a contaminated site has been mostly destructive. For decades, soil borings and groundwater wells have been used as the only techniques to gain information about the condition of the contamination. Even though destructive methods are actually capable of providing data about the amount and characteristics of the contaminant at single points, they are very costly and ineffective in determining the extent and the location of a plume (Van der Roest et al.). With GPR, survey can be completed more quickly, thereby presenting a more cost – effective surveying approach.

GPR surveys being non –invasive and non destructive can be seen as an environmentally friendly means of mapping the sub-surface and by so doing can help environmental engineers as well as geophysicists to identify the source and boundaries of contaminant plumes and as well as provide other useful geological information.

Ground penetration radar uses no radiation and emits no radiation. As a result of this advantage, there is no need to clear workers from any area because there are no negative effects of radioactive materials and hence GPR can be viewed as a safer way of obtaining data.

Unlike other methods, GPR can be completed quickly. Thus, reducing the time needed to do a survey. Also, with the advent of advanced systems having onboard computers which facilitate data processing while acquiring high – resolution continuous survey data that can be interpreted qualitatively thereby making it able to operate in a real – time mode and hence avoiding the film developing times. GPR scans are also readily available within minutes.

Furthermore, the combined software utilisation of post-processing filters, small survey paths and the 3-D function enables a clear interpretation and presentation. This tends to make final report user-friendly which goes a long way to afford the client an understanding of the investigation results that can be presented at an in-house level.

Another important advantage of GPR survey technique its simple instrumentation set – up and portability. This means that no physical contact between the transmitter and receiver antenna and the subsoil is necessary. This is in contrast to other technique such as seismic where extensive equipment location planning and physical installation is required. With GPR the transmitter and receiver antenna can be place on a cart or carried over the survey area with data acquisition occurring immediately and requiring only one person for the entire data collection process.

The integration of GPS with GPR also provides accurate determination of the measurement location while the survey is in progress thereby eliminating the need to mark off a well-defined grid on the survey site and allowing rapid geophysical survey data collection over large areas.

Lastly, Comparing GPR to other geophysical surveying methods, GPR provides the broadest range of geological feature detection; including glaciers, sediment thickness, bedrock, fractures, faults, groundwater, voids and sinkholes.

2.5 Applications of GPR

Since the first ground penetrating radar survey was performed in Austria in 1929 to sound the depth of glacier, applications of ground penetrating radar have expanded in an inconceivable pace. GPR system manufacturers estimate that there are thousands of systems around the world, however, GPR has a wide range of applications and has been properly applied to a variety of problems from archaeology to geology, quarry, environmental, engineering, mining, and many other different applications. Below are some of the applications of GPR in some fields:

2.5.1 Archaeology

2.5.1.1 Concordia Temple in Agrigento, Sicily

GPR survey was applied to the Concordia Temple in Agrigento, Sicily due to its potential to reconstruct buried structures in 3 - dimension.



Figure 2.5 Concordia Temple in Agrigento, Sicily

Radar data of the Concordia Temple were collected in an effort to help define the construction techniques used by the Greeks at this location in Sicily. The GPR result showed an alternating structure of short, flat reflectors located at approximately 50ns in the peristyle and a continuous horizontal reflector at approximately 35ns within the inner part of the temple (the cell). These results indicate that it may be necessary to modify the original hypothesis regarding the construction technique employed in the temple, as the radar data does not support the idea of a retaining wall built of completely artificial grout material. The 2D and 3D images indicate, instead, that typical construction techniques of the classical Greek period were used, which involved exploiting the surrounding landscape to obtain foundations (artificial and natural) capable of supporting such monumental and stately buildings.

This research has shown the validity of this technique to investigate the foundation geometry of any kind of archaeological building where it is not possible to apply a destructive technique. (Barone et al 2007)

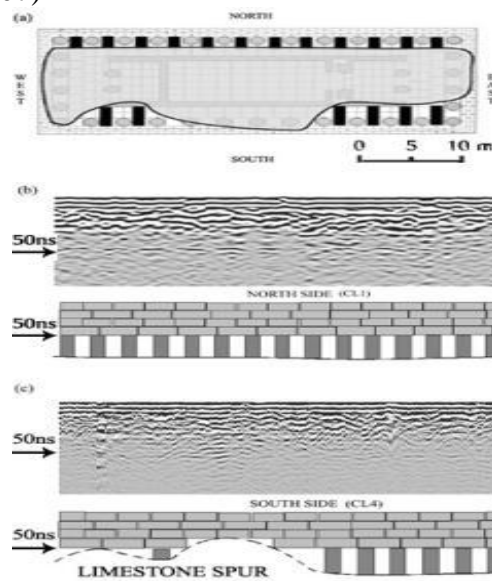


Figure 2.6 Schematic map showing the location of the 261m of GPR data collected relative to the visible structure of the Concordia Temple on the left and on the right is (a) Schematic reconstruction of the plan of the temple, (b) the northern longitudinal section and (c) the southern longitudinal section, based on the acquired GPR data.

2.5.1.2 Structural Control of Historic Buildings

Preservation of historical buildings requires particular care, as any intervention must not alter or damage the style, structure or contents of the edifice. In order to properly plan the restoration of a building, non-destructive techniques can be used extensively to detect structural elements and weaknesses. Ground-penetrating radar (GPR) is particularly well adapted to this type of work, as the method is non-invasive, rapid and provides high-resolution images of contrasting subsurface materials. (P.M.Barone et al 2010)

The aim of this work is to investigate two historic building that differ in age, structure and geometry. Also, to detect fractures and internal lesions in the architrave of the Porticus Octaviae and to determine the internal structure above the vaulted ceilings that host a series of 16th century frescos in the Zuccari Palace.

Lastly, to develop the best possible protection plan, retrieving quantitative information about the location and the dimension of the lesions as well as the thickness of the different layers.

These two historic buildings (Porticus Octaviae and Zuccari Palace) are located at downtown Rome, Italy.



Figure 2.7: The archaeological site of Porticus Octaviae (left) and the poor state of conservation of marble of the Porticus Octaviae (right)



Figure 2.8: A general view of the Zuccari Palace

GPR data processed into 2D and 3D GPR from both sites using Ekko View Deluxe and Ekko Mapper 3 is illustrated on the following radargrams.

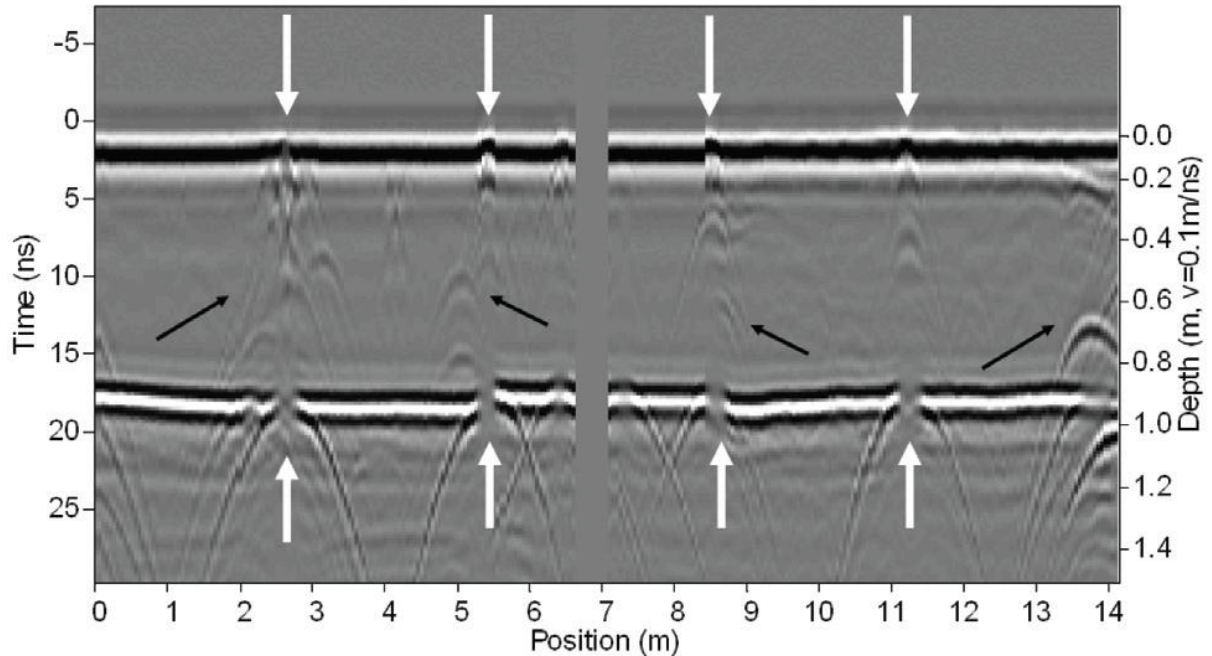


Figure 2.9: GPR section conducted using the 500 MHz antennas along a 14 m long line across the architrave of the Porticus Octaviae. No processing has been applied to this data. This section clearly shows the areas of inner lesions (black arrows) and the filled fractures that penetrate through the entire architrave (white arrows).

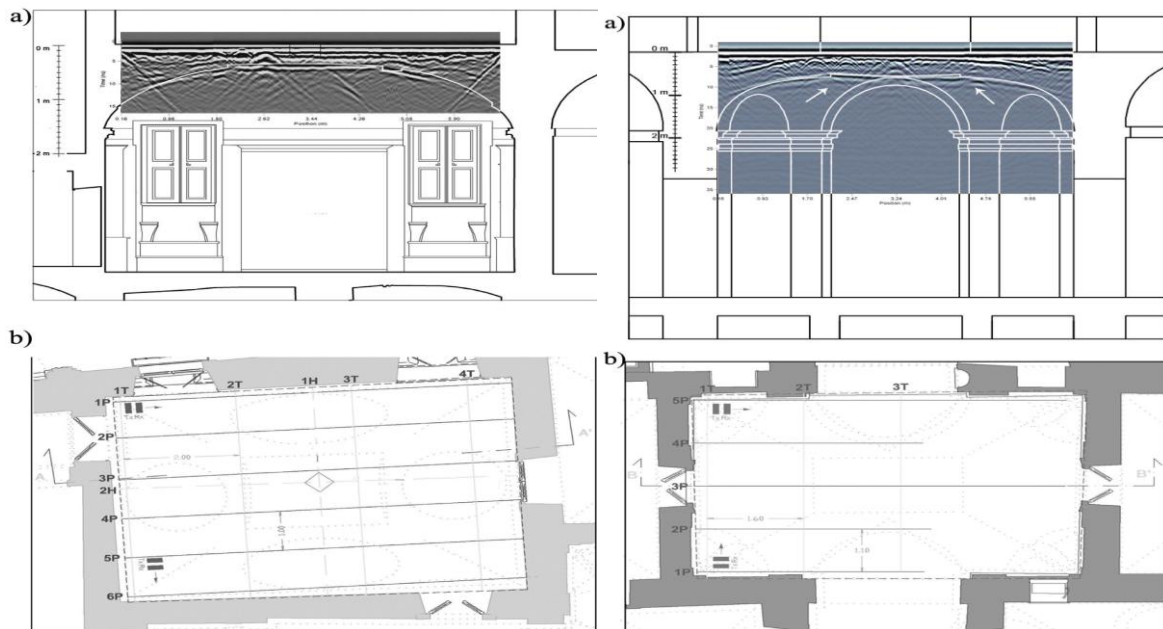


Figure 2.10: Radargrams showing the internal geometry of the vaulted ceiling in the Zuccari Palace.

From the radargram of the Porticus Octaviae, at the marble/air interface, there are strong hyperbolas indicating fractures which are visible on the surface of the marble and also their extension through the marble.

The hyperbolic events are due to cracks or fractures present between or inside the edge bricks, however the two symmetrical hyperbolas, highlighted by the arrows, are generated by the corners of a rectangular bas-relief located in the middle of the vault of the Zuccari Palace. (P. M. Barone et al 2010)

2.5.2 Environmental

2.5.2.1 Mining

GPR has a widespread use in mining. GPR can detect changes in rock type and sense major structures such as fractures, faults and joints. Specific applications include defining geology structure, mineral exploration, overburden thickness determination, mine site evaluation, tunneling design, rock mass stability, placer deposit grading and ore zone delineation. GPR is also used in mineral exploration worldwide. The most common use is exploration for fluvial deposits of gold and diamonds as well as beach deposits of titanium and iron-rich heavy minerals. Other GPR uses include detection and tracking of mineral-rich veins, major fault zones, and lateritic nickel exploration (www.senssoft.ca)



Figure 2.11: Uranium exploration in Africa on left and Kimberlite exploration in Tanzania on the right

2.5.2.2 Quarry

Extraction of rock for building stone requires the selection of sound and workable rock. The ability of ground penetrating radar to detect structure integrity and undesired jointing and cracking prior to extraction deliver major economic benefit. Marble, granite and limestone quarrying operations worldwide use GPR for critical development decisions (<http://www.senssoft.ca>)



Figure 2.12: Building/Dimension Stone Integrity

2.5.2.3 Unconventional Deep-water Investigation of Drilling Obstructions.

GPR was used at the Walter F. George dam rehabilitation drill site to assess the extent of a metal obstruction within limestone bedrock beneath almost 100 feet of water. The obstruction, thought to be pipe casing, was encountered during the emplacement of a concrete pile cutoff wall. The metal had been removed by excavation to a depth of 20 feet and the excavation filled with concrete, but further drilling encountered additional metal. The problem was to determine if the metal persisted at depth. (Hager et al, Anon).

The survey was designed for an underwater investigation on the lake bottom using the Tubewave-100 borehole radar antenna. GPR investigations were conducted to locate rebar in concrete.



Figure 2.13: A lock at the Walter F. George Dam.

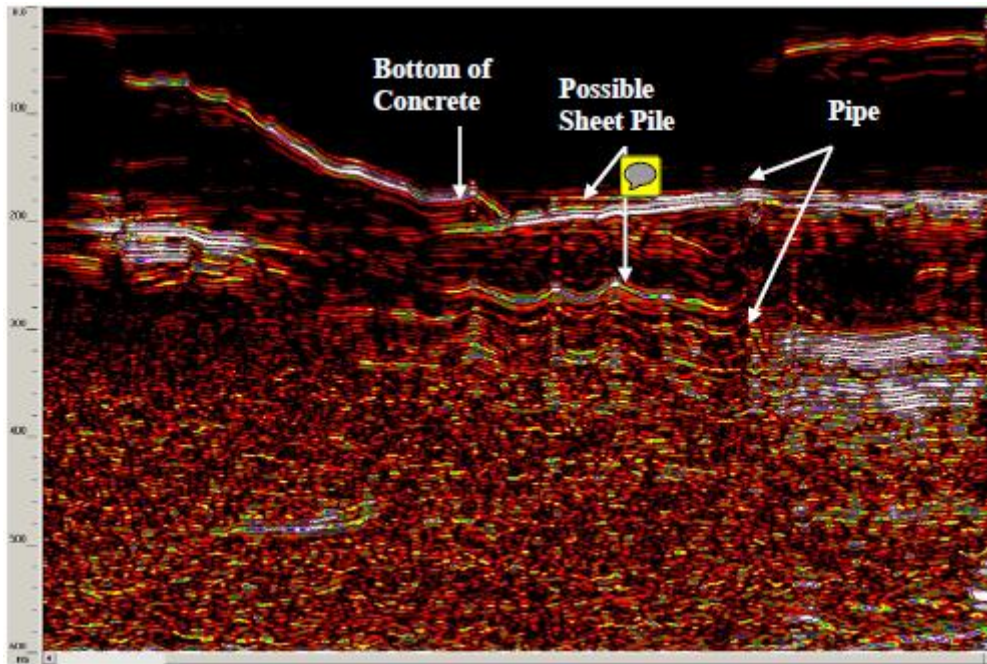


Figure 2.14: Processed GPR record for data collected

The unconventional GPR investigation using Tubewave-100 was able to map features on the lake bottom at 95 feet (29m) of water. It was resolved that pile 187 should be abandoned and cut off wall extended around it.

2.5.3 Engineering

GPR has widespread applications in the field of engineering too. For example, it can be used in concrete engineering to provide information concerning rebar spacing, placement, depth of coverage and concrete thickness. A rebar is a common steel bar, and is commonly used as a tensioning device in reinforced concrete and reinforced masonry structures holding the concrete in compression. Historically, this work was performed using X-ray, and involved working outside regular hours. It also involved evacuating large areas, arranging for special security and safety precautions and then dealing with radioactive material. GPR has been used in doing the same work; for example in active hospitals, schools, and shopping centers with no need to evacuate, during crowded open hours.

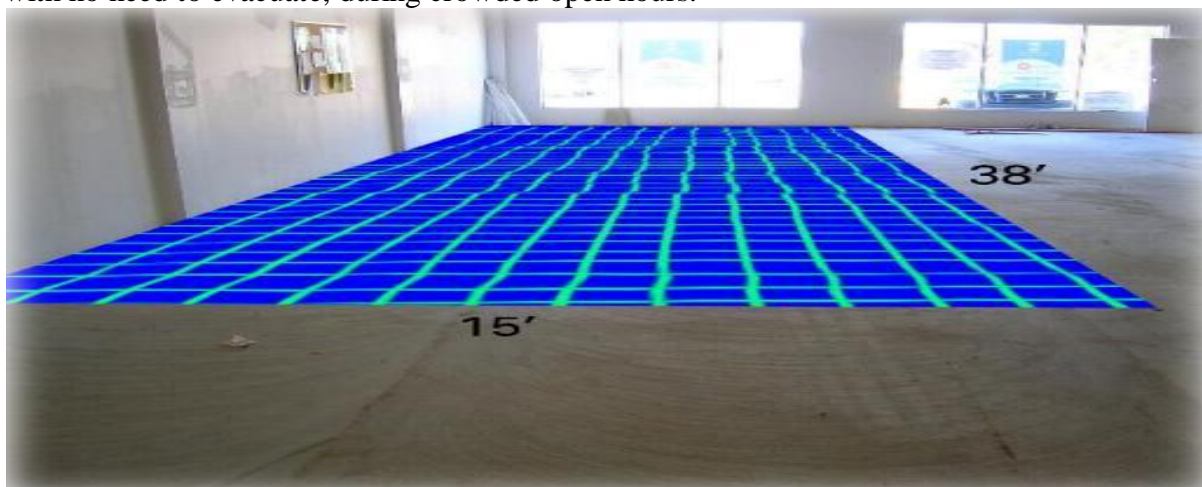


Figure 2.15: GPR image showing rebar spacing and thickness

In addition to, GPR can be used in void detection. GPR can distinguish between slab-on-grade and suspended slabs. Therefore we can locate voids beneath concrete pads. These voids may be the results of inadequate compaction during construction, washouts or erosions. The information can then be tied into site plans and additional analysis and corrective actions can be performed.



Figure 2.16: Void in concrete on the left and GPR image of void in concrete on the left

2.5.4 Forensic uses

2.5.4.1 Location of Human Burials

GPR has been successfully used to locate human burials of marked and unmarked human burials in historic and pre-historic cemeteries and in forensic work. The location of graves with GPR can be accomplished in many ways. These include locating disturbed soil associated with the grave shaft, reflections associated with bones, coffins, grave goods, clothes and the detection of breaks in the natural soil stratigraphy. The location of disturbed soil associated with a grave is perhaps the most distinctive feature of a burial. The mixing of soil due to excavation causes changes in the porosity, leading to changes in the electrical and magnetic properties of the material, all of which create radar reflections differing from the surrounding subsoil. Burials can also be located by locating breaks in the natural soil stratigraphy. The bones, clothing, coffin, coffin hardware and grave goods are possible radar reflectors. A strong reflection may be caused by the skull due to the air void within. It has also been suggested that the decomposition of human remains leach calcium salts into the surrounding subsoil for many years. These salts change the electrical properties of the surrounding soil, making it visible to radar waves. (www.archaeophysics.com)

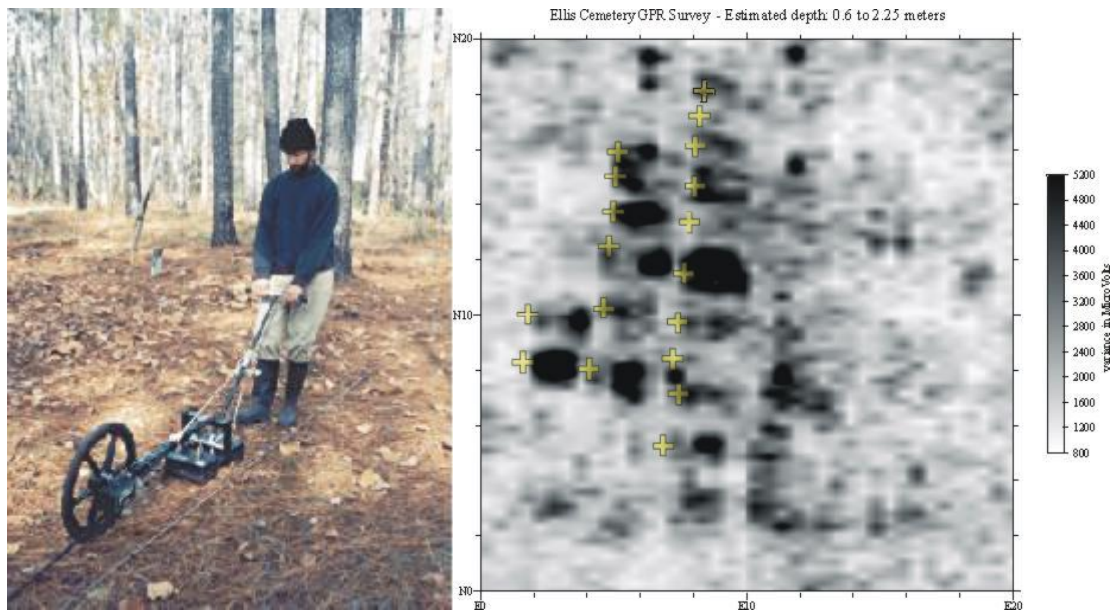


Figure 2.17: GPR in use on an historic cemetery (left) and A Time-sliced GPR map of a 19th century cemetery showing correlation between geophysical anomalies and existing grave markers (shown in yellow) (right).

GPR data processed produced a time-sliced GPR map of the cemetery that showed correlation between geophysical anomalies and existing graves marked in yellow. Forensic use of GPR is useful in investigating of archaeological and investigative events.

2.6 GPR Instrumentation

Ground penetrating radar uses a variety of technologies to generate the radar signal. The technologies include impulse, stepped frequency, Frequency-modulated continuous wave (FMCW).

Impulse ground penetrating radars on the reflected energy as a function of time. Its components consists of an emitter of that emits high frequency waves in the microwave band (either Ultra High Frequency or Very High Frequency), and a receiver which detects and amplifies the reflected and scattered waves. Impulse radars normally have low cost parts and generate simple impulse waveform. As a result of this, they are commercially powerful but however, they have one major disadvantage with regards to the resolution of the image. The resolution of the imaging depends on the width of the pulse that is used. This means that the resolution of the imaging is restricted by the width of the pulse that is used. Impulse ground penetrating radar is broadly used in data collection techniques; whether it is in the time or frequency.

Another type of ground penetrating radar is the Frequency Modulated Continuous Wave Ground Penetrating Radar. These types of radars acquire and continuously transmit data on the reflected energy as a function of frequency. The technique here is the transmission of a frequency sweep over a fixed bandwidth such as from a beginning to an end frequency. The reflected waves are mapped with regards to the frequency and as a result, are a measure of the energy that has been scattered from the objects in the subsurface.

In addition to the two aforementioned types of ground penetrating radars, there is another type called the Stepped Frequency Ground Penetrating Radar. This type of GPR transmits

data on reflected energy in a stepped linear increment over fixed bandwidths. That is, the frequency of each signal in the waveform is linearly increased in discrete frequency steps, by a fixed frequency step. These types of GPR radars are very powerful. This is because large bandwidths are needed in ground penetrating applications to locate, detect and identify subsurface features. Furthermore, in order to eliminate the problem of weaker signals from deeper targets being covered by stronger signals, compensation is made for lateral scattering and taking notice of the unambiguity in the range that can be measured by the stepped frequency radar.

There is also a special kind of GPR that uses unmodulated continuous-wave signals. This is holographic subsurface radar that is different from other ground penetrating radar types in that it records plan-view subsurface holograms. The depth penetration of this kind of radar is very small (up to 20-30 cm), but lateral resolution is enough to differentiate different type of landmines in the soil or cavities, defects, bugging devices, or other hidden objects in walls, floors and structural elements.

Other variations of ground penetration radars are ultra wide band radars, synthetic aperture radars, noise source radars and arbitrary waveform radars. Some custom ground penetration radars may also be designed, such as borehole radars. (www.ehow.com)

2.7 State of the Art of GPR

2.7.1 Introduction

GPR is a relatively young geophysical technique. Over the years, there has been tremendous and rapid improvement in this field. Data acquisition, processing and inversion as well as data interpretation have significantly improved. Brands such as GSSI, Mala, Noggin and pulse EKKO, etc have done in depth research on GPR and have produced more modern and sophisticated types to meet the challenges of the geophysical field today. These brands have post processing software which is compatible with modern and latest version of operating systems-windows 7. The GSSI uses RADAN while the Noggin and pulse EKKO uses EKKO View and EKKO Mapper.

2.7.2 How modern is Noggin and PulseEKKO?

In early GPR systems, elements that made up a GPR system were individual components that the operator had to assemble and interconnect. Now, Noggins are complete Ground Penetrating Radar (GPR) systems crafted into a single package providing high performance and ease-of-use. By design, Noggin systems can operate in a wide range of environments and in extreme temperatures or weather conditions. The system has been designed such that they are lightweight. The lightweight units can easily be move from location to location and use quickly deployable configurations to reduce setup time and allow for rapid surveying. There are also peripherals like optical encoded odometers and GPS support that provide accurate positioning when surveying. There is also a new technology called spider that allows networking together any number of Noggin and pulse EKKO PRO GPR units to create virtually any multi-channel GPR deployment imaginable.

Noggins have the following state of the art types of GPR which is employed at different areas. They are SsmartCart, SmartHandle, SmartTow and Rock Noggin.

The SmartCart quickly cover large flat open areas such as lawns, roads and sidewalks.



Figure 2.18: An operation making acquisition with a SmartCart GPR.

SmartHandle operate on smooth vertical or overhead surfaces and in confined spaces where early GPR systems could not operate.



Figure 2. 19: SmartHandle GPR being used by a military for data acquisition.

SmartTow operates in rough areas where towing is practical.



Figure 2.20: SmartTow in operation.

Rock Noggin surveys rough or hard-to-access areas such as mines, tunnels, rock faces etc.



Figure 2.21: Rock Noggin GPR being used on hard rock and inside a tunnel.

2.7.3 Noggin and PulseEKKO Software

EKKO_Mapper and EKKO_Interp are software used by Noggin operators to analyse the data acquired by the Noggins and pulseEKKO GPR. Unlike early software, the new ones have simple and intuitive interface. Also, they support current operating windows which make it easy to be installed and used by the operator. They also have simple features such as points, polylines, boxes and annotation together with automatic or user-defined properties like colours, style, markers and marker size which make it easy to distinguish between them.

The new software is flexible in that it allows the user to easily add, move, delete and insert features. Also, interpretation is not strict to a single cross-section image; they can span multiple images. The software saves the image file in extension such as JPG, BMP, TIF which are easily included in reports or import into other software like GIS software.

2.7.4 Improvement in GSSI

2.7.4.1 The Past, Present and Future of GPR Antennas

With nearly four decades experience, there has been significant improvement in GSSI design of GPR antennas and other accessories. Presently, GSSI antennas feature the highest signal-to-noise ratio of any antenna available in the industry, providing the highest quality of data with clear and accurate results.

There are a series of antennas developed by GSSI to meet the needs of a broad range of applications. All antennas are interchangeable with any of the GSSI accessories (SIR-system). The following features make GSSI GPR instruments meet the state of the art in the geophysical investigations field of today.

- Rugged, military-style connectors
- Long-life replaceable wear skirts
- Coated, sealed electronics
- Rugged, high-density molded cables
- Shielding to eliminate aboveground interference
- Operates from -20°C to 50°C

Table 2. 2: GPR central frequency, depth of penetration and applications.

Center Frequency	Depth of Penetration	Typical Applications
2600 MHz	to 0.4 m	Concrete Evaluation
2000 MHz Palm	to 0.4 m	Concrete Evaluation
1600 MHz	to 0.5 m	Concrete Evaluation
1000 MHz	to 0.6 m	Concrete Evaluation
900 MHz	0-1 m	Concrete Evaluation, Void Detection
400 MHz	0-4 m	Utility, Engineering, Environmental, Void detection
270 MHz	0-6 m	Utility, Engineering, Geotechnical
200 MHz	0-9 m	Geotechnical, Engineering, Environmental
International		
100MHz	2-15 m	Geotechnical, Engineering, Mining
16-80 MHz	0-50 m	Geotechnical
Air- Launched Horn		
1.0 GHz	0-.75 m	Pavement Thickness and Road Condition Assessment
2.0 GHz	0-.9 m	Highway and Bridge Deck Evaluations

Depth of penetration may vary depending on soil conditions.

GSSI has in its fold the following ultra modern GPR instruments designed purposely for specific geophysical area. They include:

- The Profiler

- SIR-20
- SIR-30
- SIR-300
- Structure Scan Mini
- Structure Scan Optical
- Structure Scan Standard
- Road Scan
- Bridge Scan
- Utility Scan

The Profiler system is a multi-frequency electromagnetic (EM) conductivity meter made up of two main components:

1. EM instrument; which is comprised of the transmitter, receiver and electronics enclosure
2. PDA; the instrument interface



Figure 2.22: The Profiler in use.

The Profiler can be applied in the following geophysical fields:

- Environmental assessment
- Archaeology
- Geological investigation
- Site assessment
- Ground water investigation
- Agricultural research

Data acquired by the Profiler has a user-friendly system, unmatched signal stability and multi-frequency system.

Also, the Profiler has premium mobility ability. This is because it is lightweight-weighs under 4.5kg, has a wireless data logger that eliminates cable noise, has integrated GPS and environmentally sealed system that is durable and east to transport.

The Profiler delivers real-time results and also files of the result are stored on internal memory and structured in Excel format.

The Profiler has versatility and functionality features. It is a frequency domain, electromagnetic profiling system hence by acquiring multiple frequencies; the user can select the frequencies that provide the best results for a specific application.

The Profiler system has mechanical structure and electronics designed for maximum structural and thermal stability. These key features minimize signal drift and maintain an accurate zero level and system null across the full bandwidth of the system, whereas signal drift is a common problem with traditional EM instruments.

The SIR-20 is a rugged, high-performance dual-channel GPR data acquisition system coupled with a rugged Panasonic ToughBook PC. The data acquisition and processing is based on Microsoft Windows. This provides the user with a familiar operating environment for collecting, storing, processing and transferring data. There are specific processing functions that enable the user to present the interpreted GPR results in practical, useful formats.

The SIR-20 is compatible with all GSSI antennas, allowing the user to address the full range of GPR applications. Whether mounted on a vehicle, a cart-based system or mobile on-site, the SIR-20 will provide the highest quality data, all the time.



Figure 2.23: GSSI SIR-20 inspecting a bridge deck.

Typical Uses

- Road structure assessment
- Bridge deck inspection
- Rail bed inspection
- Concrete inspection
- Archaeology
- Geological investigation
- Mining

The SIR-20 has the following features that make it more modern than the early ground penetrating radars.

Flexible design-has dual channel system-collect data using any two GSSI antennas and also connected with a rugged Panasonic ToughBook computer which provides familiar Windows environment.

It also has integrated system- ideal for vehicle mounted applications-operates in either 120 volts AC or 12 volts DC. There is also GPS compatible.

It is also able to store large data and has USB port for system flexibility.

The SIR-30 is a rugged, high-performance multi-channel GPR data acquisition system. This control unit can collect up to four channels of data simultaneously with uncompromised performance.

The SIR-30 offers advanced filters and display capabilities for real-time processing including migration, surface positioning, signal floor tracking and adaptive background removal.

As the basis of a high-speed data collection system, the SIR-30 is ideal for: measuring pavement layer thickness, detection of cavities, airport runway assessment, detection of fouled/ clean ballast and utility detection.



Figure 2.24: SIR-30

Typical uses include

- Road structure assessment
- Utility designation
- Bridge deck inspection
- Rail bed inspection

Features of the SIR-30 include:

- Flexible and modular design
- Available in a two or four channel configuration
- Operate the control unit with a laptop computer or as a standalone system
- Compatible with all GSSI antennas integrated system
- Ideal for vehicle-mounted applications, supports AC or DC operation
- Full internal GPS loggings capability
- Multiple mounting configurations deliver results

- High speed GPR data collection-capable of more than 1,375 scans/seconds, per channel
- Up to 500 GB data storage
- USB/ Ethernet/ compact flash ports for system flexibility

The SIR-300 is a rugged, high-performance single- channel GPR data acquisition system. It is the industry's number one choice for data accuracy and versatility. This small, lightweight control unit is designed for single-user operation. It has all the essential features and flexibility that experienced GPR users require, as well as simplified, application-specific user interfaces for novice GPR users.

The SIR-3000 incorporates advanced signal processing and display capability for 'in-the-field' 3D imaging. Unlike other data acquisition products on the market, the SIR-3000 is interchangeable with all GSSI antennas, making it an affordable and flexible option for multi-application users.



Figure 2.25: SIR-300 being used to inspect a tunnel.

Typical uses of SIR-300 include:

- Concrete inspection
- Utility location
- Geological investigation
- Archaeology
- Forensics
- Bridge deck inspection
- Mining
- And many other custom applications

Other modern features of the SIR-300 include:

- Modular design
- Compatible with all GSSI antennas
- Lightweight and portable
- Removable, rechargeable batteries integrated system
- Windows-based user interface

- GPS integration
- High-resolution colour screen that is visible over a wide range of light conditions
- Rugged and weather resistant deliver result
- Removable compact flash card memory
- Large internal data storage

The StructureScan Mini is ideal for locating the position and depth of rebar, conduits, post-tension cables, and voids in up to 0.5m of concrete. The high resolution, LED backlit 5.7” display provides a detailed image of the subsurface structure. In addition to viewing, the data image can be stored directly to a SD-RAM card for later playback, or transferred to a computer for printing or integration into a report.

The StructureScan Mini is lightweight, weighing in at just over three pounds. The small size of the unit makes it easy to transport to the job site and once on site, convenient to scan around obstacles and into tight spaces. The Mini is very easy to use – new users will become proficient in a few short hours. The Mini aids in target detection by marking the data on screen with a small dot when a rebar or a conduit is identified. The lasers on the side of the unit indicate the exact location of the center of target for accurate marking prior to cutting or coring.



Figure 2.26: StructureScan Mini.

The StructureScan Mini has the following features that make it meet the modern state of art of geophysical instruments.

- All-in-one handheld GPR system
- Ergonomic handle and controls

- Easy to use operator interface with colour display screen
- Survey wheel with encoder
- Guiding laser for locating

It also has a compact design features that makes concrete inspection easy in tight spaces. Again, it has integrated tool feature i.e. all-in-one concrete inspection tool-antenna, positioning system and control unit combo. System is flexible because the StructureScan Mini is offered in two versions, the original system that generates 2D data (distance, depth), or the new system with 3D (length, width, depth) capabilities. It is durable since it has ruggedized plastic casing and wheels for long-lasting performance.

StructureScan Mini Viewer is software ideal for basic post processing of 2D StructureScan Mini data files. The software has features that include: gain (contrast) control, background removal, colour table and save/ convert to images.

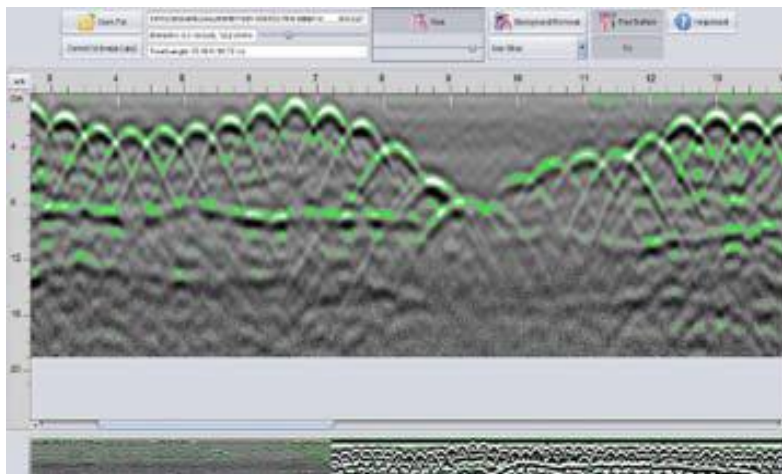


Figure 2.27: Radargram produced by the StructureScan Mini Viewer.

Another post processing software that the StructureScan Mini Series uses is the RADAN. It is designed to process, view, and document 2D data collected with the StructureScan Mini. RADAN for StructureScan Mini can perform the following functions:

- Copy images to third party software for documentation purposes
- Save images
- Print to all Windows supported printers
- Background Removal filtering
- Establish Ground Truth for near accurate depth calculation
- Dielectric calculation
- Colourize the data
- Add targets and export target information in an Excel format
- Gain (contrast) control

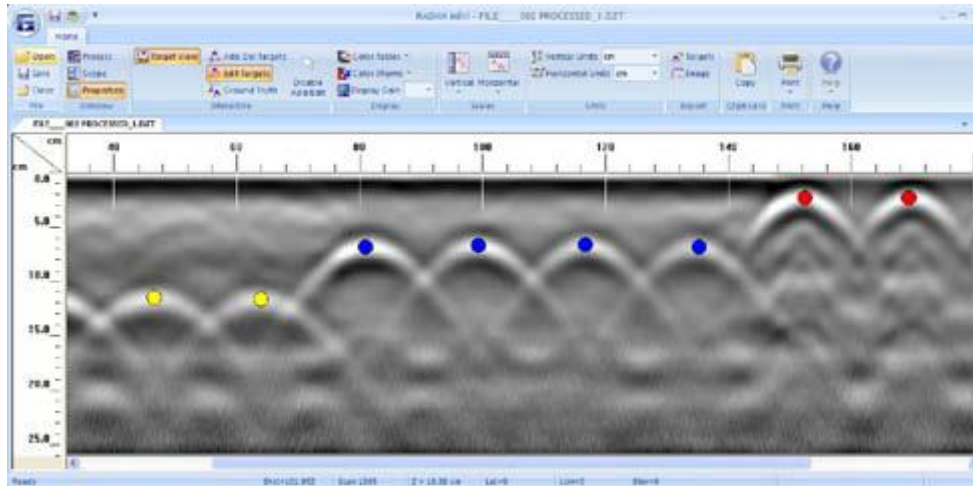


Figure 2.28: Radargram produced with RADAN software.

StructureScan Optical StructureScan Optical has revolutionized 3D data collection by simplifying an often complicated survey process while providing the most versatile GPR solutions in the industry.

StructureScan Optical is the only concrete inspection tool on the market with optical barcodes and patented Smart Pad technology for simple error-free scanning.

Typical uses include:

- Concrete inspection – locate metallic and non-metallic targets in walls, floors and ceilings
- Structure inspection – bridges, monuments, towers, tunnels, garages, parking decks and balconies
- Condition assessment – map relative concrete condition for rehab planning
- Measure slab thickness
- Void location

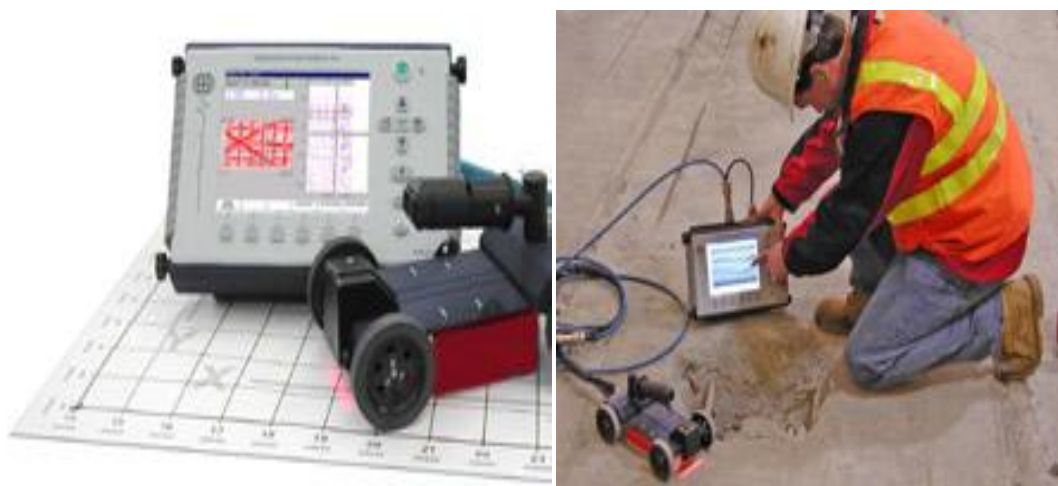


Figure 2.29: StructureScan Optical in operation

The StructureScan Optical has the following features:

- Locate targets
- Real-time data collection

- Obtain accurate GPR data result on concrete structure
- Locate rebar, tension cables, conduits (PVC and metal) in real-time
- Ability to cross-polarize antenna for additional data in locating PVC and conduit acquire data
- Data is displayed in simple planview on a high-resolution, colour screen
- Instant 3D data collection Result
- Simplify data collection using Smart Pads with optical bar codes
- Varied data collection pad sizes offer maximum flexibility

The StructureScan Standard system provides a non-destructive means to accurately inspect concrete structures. StructureScan Standard is used to safely locate embedment within concrete structures prior to drilling, cutting or coring.

Typical uses for StructureScan Standard include:

- Concrete inspection-locate metallic and non-metallic targets in walls, floors
- Structure inspection-bridges, monuments, walls, towers, tunnels, balconies, garages, decks
- Condition assessment- map relative concrete condition for rehab planning
- Measure slab thickness
- Void location

The features that make StructureScan Standard more modern are as follows:

- Locate targets
- Locate rebar, post-tension cables, conduits (PVC and metal)
- Surveys up to 18 inches in depth
- Establish and mark targets in real-time with back-up cursor feature integrated system
- Windows – based user interface
- Data is displayed on a high-resolution, color screen
- Ability to save data internally Premium Mobility
- Rugged handcart-based system that is lightweight and simple to transport
- No site hazards or need to close of work areas as with radiography (X-Ray)



Figure 2.30: StructureScan Standard inspecting concrete wall.

The RoadScan system is an effective GPR tool for quickly determining pavement layer thickness. RoadScan is able to collect data densities not obtainable by traditional labor-intensive methods such as coring. RoadScan data can be acquired at highway speeds, which eliminate the need for lane closures and provide a safer working environment.

The GSSI road antennas are air-launched at a height of 0.5m hence it work perfectly on rough roads. It is a multi-channel hence two antennas can be used simultaneously for data collection. RoadScan system delivers results in a form of ASCII as an output files that makes transfer to other software programs easy and simple. The results output as Google Earth is in klm file extension.



Figure 2.31: Single (left) and multiple (right) mount antennas RoadScan inspecting road.

Traditional bridge deck inspection methods, like hammer soundings and chain dragging, rely on a person to interpret acoustical feedback to determine good and bad areas of concrete. Existing asphalt overlays must be removed prior to using these methods, and results vary depending on the operator's technique and interpretation of results.

The application of BridgeScan GPR provides accurate condition assessment of bridge decks as well as other reinforced concrete structures. Hundreds of bridge decks have been evaluated using GPR.

BridgeScan is a complete, affordable GPR system that provides an effective tool for quickly determining the condition of aging bridge decks, parking structures, balconies and other concrete structures. The system is also used to obtain accurate concrete cover depth on new structures and void detection and location. With BridgeScan, repair costs can be estimated correctly, saving time and money.

The BridgeScan GPR has the following features that make it meet the modern state of the art of geophysical instruments. These include how it acquires data and process it and how it delivers results. It is a convenient self-contained cart-based design integrated with GPS. The system is integrated with specially designed software to post process the GPR bridge data in order to account for bridge skew angle.



Figure 2.32: BridgeScan GPR assessing bridge deck, reinforced concrete (left) and road structure (right).

GSSI UtilityScan is industry standard ground penetrating radar for locating and mapping subsurface utilities. UtilityScan users can quickly identify and mark the location and depth of services utilities such as gas, communications, sewer lines and other metallic and non-metallic targets including underground storage tanks and PVC pipes. It is also typically used in environmental remediation, geological investigation and archaeological and forensic investigations.



Figure 2.33: UtilityScan locating and mapping underground utilities.

Features of UtilityScan:

- Designate targets
- Real-time data collection
- Back up cursor allows the user to accurately locate targets premium mobility
- Easy to transport
- Durable components tested to withstand the toughest conditions integrated systems
- Windows operating system
- Ability to store and replay data
- GPS integration value
- Multiple antenna options
- Flexible system for concrete and bridge inspection applications

Early time ground penetrating radars do not possess all the above features of the GSSI UtilityScan hence much improvement has been seeing in the field of geophysical instruments.

2.7.5 MALÅ GPR

Another brand of ground penetrating radar (GPR) that has seen tremendous improvement over the years is the Australian MALÅ. MALÅ GPR (ground penetrating radar) is the most versatile geophysical technique, used in wide variety of near surface application areas. Even though physical properties of the subsurface will limit resolution with depth, MALÅ GPR (ground penetrating radar) remains as the unmatched champion of high resolution subsurface profiling, object detection and mapping. MALÅ GPR (ground penetrating radar) is generally used for investigations of the subsurface down to roughly 30 meters depth, but in favorable media the technique may penetrate several hundreds of meters.

MALÅ has features that make users benefit greatly. Some of these features include its versatility, high speed data acquisition, portability and ease of use and most importantly, the optimization of resources- one man replacing a large field crew. The main products of

MALÅ are the MALÅ MIRA System, MALÅ X3M System and the MALÅ ProEx System. These ultra modern products have in-built features that make them meet the current state of the art and challenges of the geophysical world.

Early GPR system lacked a lot of features in the imaging of the subsurface. When deploying ordinary GPR systems, the results suffer from lack of real 3D capabilities i.e. the line spacing in the surveys will, for practical reasons, be too large, meaning that information loss are inevitable.

Also, reliable positioning of detected target cannot be made easy, neither in the data acquisition process nor in the reporting phase of a typical project. The MALÅ MIRA (Malå Imaging Radar Array) Systems are the first commercial systems designed to overcome these limitations.

As opposed to other commonly marketed multi-channel systems, which in many cases could be regarded as parallel single channel systems, the MALÅ MIRA system enables fast and true 3D data acquisition. From a user perspective this means that large areas can be mapped without loss of information and that the method is suitable for almost any kind of, shallow, subsurface investigations, i.e. targets with arbitrary shape, layers and linear objects are mapped equally well.



Figure 2.34: Mala Mira GPR.

The X3M integrated radar control unit from MALÅ is compatible with MALÅ's 100, 250, 500 and 800 MHz shielded antennas and designed to fit directly onto the antenna. This combined with the built-in electronic design, low weight and compact size make the X3M one of the smallest GPR systems available.

An Ethernet link between the X3M and the XV Monitor, or Notebook PC, offers high speed point to point communication for reliable and high quality data transfer. The built-in auto stacking feature ensures optimum data quality at maximum survey speed.

It has a low power consumption rate hence it offers in excess of six hours measuring time with a standard battery.

The convenience of this flexible and modular design means that an X3M based GPR system can be quickly and easily configured for use across a wide range of applications, simply by changing the antenna. This flexible approach offers you an affordable choice to system configuration

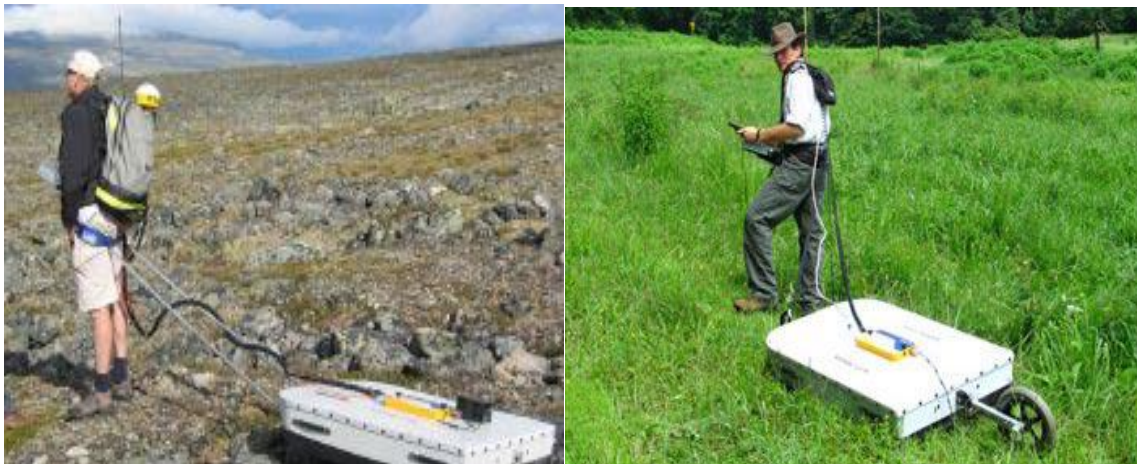


Figure 2.35: MALÅ X3M in operation on rough terrain and on grass.

The Professional Explorer (ProEx) System from MALÅ is a modular, full-range Ground Penetrating Radar (GPR) system designed to meet the needs of the advanced professional user. At the heart of this system is the ProEx Control Unit. Designed on a completely new technical platform, the ProEx is the most versatile control unit in the MALÅ range and replaces the World famous RAMAC/GPR CUII as the new high-end full range system.

The ProEx is fully compatible with MALÅ's broad range of antennas and offers a flexible and versatile approach to detecting subsurface targets and geological layers accurately, efficiently and in real-time.

MALÅ's modular design approach offers you a flexible and affordable choice to system configuration.



Figure 2.36: MALA ProEx GPR System in use to investigate the subsurface.

The Easy Locator from MALÅ is an easy to use, entry level Ground Penetrating Radar (GPR) system designed to meet your utility locating needs. The Easy Locator is the tool of choice for those who need to quickly and easily identify the presence of buried utility infrastructure, both metallic and non-metallic.

Modern advances in technology, particularly in the design and construction of buried utilities, have resulted in an ever increasing use of non-metallic materials.

The Easy locator also specific features:

- Minimal set up for fast start-up
- Quick and simple one button operation
- Real time locates
- Detects metallic and non-metallic utilities
- Back up cursor for quick and accurate utility marking
- 10.4" colour LCD screen
- Compact, portable and field rugged design – IP66
- Available in nine different languages (English, French, Italian, Spanish, German, Swedish, Norwegian, Russian and Chinese)

The product's simple yet ergonomic and field rugged design, intuitive user interface and clear display is testament to its success and it remains as the number one choice in its field.



Figure 2.37: MALA Easy Locator investigating the subsurface.

In conclusion, ground penetrating radar (GPR) brands such as Noggins and pulseEKKO, GSSI and MALÅ have seen significant improvement over the years. Features that early GPR instruments did have are now are integrated in the modern GPR. This makes modern GPR system more flexible, versatile, portable and on top technologically inclined.

3 SOIL CONTAMINATION

3.1 Introduction

Soil contamination is the presence of man-made chemicals or other alteration to the natural soil environment. The contaminants are either solid or liquid hazardous substances mixed with the naturally occurring soil. Contaminants in the soil are usually physically or chemically attached to soil particles, or, if they are not attached, are trapped in the small spaces between soil particles. This type of contamination typically arises from the rupture of underground storage tank, application of pesticides, and percolation of contaminated surface water to subsurface strata, oil and fuel dumping, leaching of wastes from landfills or direct discharge of industrial wastes to the soil. The most common chemicals involved are petroleum hydrocarbons, solvents, pesticides, lead and other heavy metals. This occurrence of this phenomenon is correlated with the degree of industrialization and intensities of chemical usage.

Soil contamination is of much concern because it directly affects human health, through direct contact with the contaminated soil, ingestion of vapors from the contaminants. Also, potentially greater threats are posed by the infiltration of soil contamination into groundwater aquifers used for human consumption, sometimes in areas apparently far removed from any apparent source of above ground contamination.

Soil contamination can also have significant deleterious consequences on the ecosystems. There are radical soil chemistry changes which can arise from the presence of many hazardous chemicals even at low concentration of the contaminant species. These changes can manifest in the alteration of metabolism of endemic microorganisms and arthropods resident in a given soil environment. The result can be virtual eradication of some of the primary food chain, which in turn has major consequences for predator or consumer species. Soil contamination also has adverse effects on agricultural lands which contain certain types of contaminants (organic and inorganic). Contaminants typically alter plant metabolism, most commonly to reduce crop yields. This has a secondary effect upon soil conservation, since the languishing crops cannot shield the Earth's soil mantle from erosion phenomena.

Some of these contaminants can be carcinogenic hence the need to map the contaminated site up and apply the right remediation technologies. Mapping of contaminated soil sites and the resulting cleanup are time consuming and expensive tasks, requiring extensive amounts of geology, hydrology, chemistry, computer modeling skills, and GIS in Environmental Contamination. Also, it is necessary to characterize the site before any mapping can be carried out. This will go a long way to give a fair and deep idea about the site under investigation. This will help in the process in order to make the mapping cost effective and save time. Under site characterization hot spots of contaminants and zone of no contaminants will be known. Through the characterization a conceptual site model (CSM) can be drawn to start the investigation of the site contamination.

3.2 Characterisation of site (soil)

Before any geophysical method will be applied to map contaminants plume in the subsurface, a fair knowledge about the site under investigation characterization, environmental laws concerning concentration thresholds have been established and this will help to know whether a site is contaminated or uncontaminated.

Laws concerning studies and methodologies for contaminated sites characterization were enacted by Ronchi on February 5th, 1997. This decree is European directive which spells out

the regulation regarding criteria, procedures and modalities for site characterization. When is soil contaminated and needs an investigation? Before this question can be answered, threshold concentrations values need to be established and set so that the concentrations level of the site under investigation can be compared to in order to make the judgment. There are two kinds of the threshold concentrations level.

- 1) Threshold Concentrations (CSC) are the level of contaminants concentrations of the environmental matrix (atmosphere, soil, subsurface, groundwater, etc) above which it is necessary to make site characterization and risk analysis.
- 2) Risk Threshold Concentrations (CSR) is the acceptable concentrations level that must be evaluated for each single case (site) through the risk analysis procedure. This means each site has got a different CSR depending on the expert.

Now, a site is said to be contaminated if at least a contaminant concentration level exceeds the CSR. Sometimes a site has the potential to qualify to be called contaminated and also needs to be investigated. Potential contaminated site is a site where at least one contaminant exceeds the CSC.

Having known the above threshold concentrations level, one can now characterize a site in order to carry out the mapping of the contaminant plume and then the clean up exercise if necessary. An active site or brownfield can be characterized by following the following steps: Firstly, production history of the site must be known. This can be achieved through direct interview of workers, examination of archives of the site operators, aerial survey interpretation and also historical investigation. This will help to have idea about the history of the industry and chemicals involve in the operational process of the industry, the location of landfill and waste allocation. Also, the production history will describe in details the site and all the past and present production activities, identifies the correlation between activities and localization, extension and contaminant type and finally describes environmental characteristics, environmental targets and propose preliminary conceptual site model for the site characterization.

With the preliminary conceptual site model, an investigation plan can be executed. The objectives of the investigation plan are to:

- Verify the existence and the level of pollution in the ground, subsoil, backfill materials, surface water, ground water and the atmosphere.
- Evaluate the volume and the presence of contamination sources and delimit the volume of the areas of the waste materials buried.
- Identify site geologic and hydrogeologic characteristics necessary to implement the conceptual site model.
- Identify the potential targets and survey its concentration of polluting substances.
- Identify the possible ways of spreading and migrating of pollutants from sources towards the possible targets.
- Gather the data necessary for the risk analysis assessment.

Achieving the above of the objectives of the investigation plan mean investigation plan result can now be represented. This will lead to final conceptual site model through which risk threshold concentration can be define through risk analysis procedure. Under risk analysis, if the concentrations level of an active site or brownfield is less than the threshold concentration (CSC) no action is needed hence no mapping of contaminant plume is also needed but if the concentrations level of the site is greater than threshold concentration (CSC)

- a) But less than the risk threshold concentration (CSR) no action or just monitor the site.

- b) And also greater than the risk threshold concentration (CSR), then the site is contaminated and mapping the contaminant plume is necessary in order to implement remediation action and process.

3.3 Types of soil contaminants

Several types of contaminants can be traced where a site is contaminated. There are two main groups of contaminants, namely organic and inorganic contaminants. Organic contaminants are organic molecular compounds based on carbon atoms with other elements such as hydrogen, oxygen, sulphur, nitrogen, phosphorous and the various halogens (Cl, Br, F, etc). Petroleum products which are mostly hydrocarbons form major part of these organic contaminants. Most of these contaminants are polychlorobiphenyl (PCB), polycyclic aromatic hydrocarbon (PAH), chlorinated solvents etc. Also, other most prominent organic contaminants which are normally from petroleum products are the Non Aqueous Phase Liquid (NAPL). These NAPL are subdivided into two groups by comparing their density to that of water. The Light Non Aqueous Phase Liquid (LNAPL) has density which is less than the density of water and the Dense Non Aqueous Phase Liquid (DNAPL) has density greater than the density of water. Also, gasoline has additives such as methyl tert-butyl ether (MTBE) and benzene, toluene, ethylbenzene, xylene (BTEX) which are all volatile organic compounds (VOCs).



Figure 3.1: Petroleum contaminated site (www.test-llc.com)

Inorganic compounds are mostly traces of toxic metals and semimetals. Heavy metal pollution is caused when such metals as arsenic, cobalt, copper, cadmium, lead, silver and zinc are exposed in an industry or mine site come in contact with water. Metals are leached out and carried into the subsurface.

Processing chemicals pollution is another kind of inorganic contamination. This kind of pollution occurs when chemical agents (such as cyanide or sulphuric acid used by mining companies to separate the target mineral from the ore) spill, leak, or leach from the mine site into nearby water bodies. These chemicals can be highly toxic to humans and wildlife. (www.safewater.org)



Figure 3.2: Ammonia nitrate contaminated site (www.hyde-env.com)

3.3.1 Light Non Aqueous Phase Liquid (LNAPL)

3.3.1.1 Introduction

Nonaqueous phase liquids (NAPLs) are hydrocarbons that exist as a separate, immiscible phase when in contact with water and/or air. Differences in the physical and chemical properties of water and NAPL result in the formation of a physical interface between the liquids which prevents the two fluids from mixing. Nonaqueous phase liquids are typically classified as either light nonaqueous phase liquids (LNAPLs) which have densities less than that of water, or dense nonaqueous phase liquids (DNAPLs) which have densities greater than that of water.

Light nonaqueous phase liquids affect soil and ground-water quality at many sites across the world. The most common LNAPL related soil and ground-water contamination problems result from the release of petroleum products. These products are typically multicomponent organic mixtures composed of chemicals with varying degrees of water solubility. Some additives such as methyl tertiary-butyl ether and alcohols are highly soluble. Other components such as benzene, toluene, ethyl benzene, and xylenes are slightly soluble. Many components (e.g., n-dodecane and n-heptane) have relatively low water solubility under ideal conditions. Physical and chemical properties which affect transport and fate of selected LNAPL compound and refined petroleum products are presented in Table 1. In general, LNAPLs represent potential long-term sources for continued soil and ground-water contamination at many sites (Huling and Weaver, 1991).

Table 3.1: Representative properties of selected LNAPL chemicals commonly found at Superfund sites (U.S.EPA, 1990), water, and selected petroleum products (Lyman and Noonan, 1990)

Chemical	Density(g/cm^3)	Dynamic Viscosity(cp)	Water Solubility(mg/l)	Vapor Pressure (mm Hg)	Henry's Law Constant (atm- m^3 /mol)
Methyl Ethyl Ketone	0.805	0.40	2.68 E+05	71.2	2.74 E-05 (2)
4-Methyl-2-Pentanone	0.8017	0.5848	1.9 E+04	16	1.55 E-04 (2)
Tetrahydrofuran	0.8892	0.55	3 E+05(1)	45.6 (2)	1.1 E-04 (2)
Benzene	0.8765	0.6468	1.78 E+03	76	5.43 E-03 (1)
Ethyl Benzene	0.867	0.678	1.52 E+02	7	7.9 E-03 (1)
Styrene	0.9060	0.751	3 E+02	5	2.28 E-03
m-Xylene	0.8642 (1)	0.608	2 E+02	9	6.91 E-03 (1)
o-Xylene	0.880 (1)	0.802	1.7 E+02	7	4.94 E-03 (1)
p-Xylene	0.8610 (1)	0.635	1.98 E+02 (1)	9	7.01 E-03 (1)
Water	0.998 (6)	1.14 (6)	----	----	----

Table 3. 2: Common Petroleum Products of selected LNAPL (Lyman and Noonan, 1990)

Chemical	Density(g/cm^3)	Dynamic Viscosity(cp)	Water Solubility(mg/l)	Vapor Pressure (mm Hg)	Henry's Law Constant (atm- m^3 /mol)
Automotive gasoline	0.72-0.76 (3)	0.72-0.76 (3)	----	----	----
#2 Fuel Oil	0.87-0.95	1.15-1.97 (5)	----	----	----
#6 Fuel Oil	0.87-0.95	14.5-493.5 (4)	----	----	----
Jet Fuel (JP-4)	~0.75	~0.83 (5)	----	----	----
Mineral Base	0.84-0.96 (6)	~0.83 (5)	----	----	----
Crankcase Oil					

Values are given at 20°C unless noted.

(1) Value is at 25°C.

(2) Value is at unknown temperature but is assumed to be 20°- 30°C.

(3) Value is at 15.6°C.

(4) Value is at 38°C.

(5) Value is at 21°C.

(6) Value is at 15°C.

3.3.1.2 LNAPL Transport through porous media

Movement of LNAPLs in the subsurface is controlled by several processes. Upon release to the environment, NAPL (i.e., LNAPL or DNAPL) will migrate downward under the force of gravity. If a small volume of NAPL is released to the subsurface, it will move through the unsaturated zone where a fraction of the hydrocarbon will be retained by capillary forces as residual globules in the soil pores, thereby depleting the contiguous NAPL mass until movement ceases. If sufficient LNAPL is released, it will migrate until it encounters a physical barrier (e.g., low permeability strata) or is affected by buoyancy forces near the water table. Once the capillary fringe is reached, the LNAPL may move laterally as a continuous, free-phase layer along the upper boundary of the water-saturated zone due to gravity and capillary forces.

Although principal migration may be in the direction of the maximum decrease in water-table elevation, some migration may occur initially in other directions. A large continuous phase LNAPL mass may hydrostatically depress the capillary fringe and water table. Once the source is removed, mounded LNAPL migrates laterally, LNAPL hydrostatic pressure is removed, and the water table eventually rebounds. Infiltrating precipitation and passing ground water in contact with residual or mobile LNAPL will dissolve soluble components and form an aqueous-phase contaminant plume. In addition, volatilization may result in further spreading of contamination.

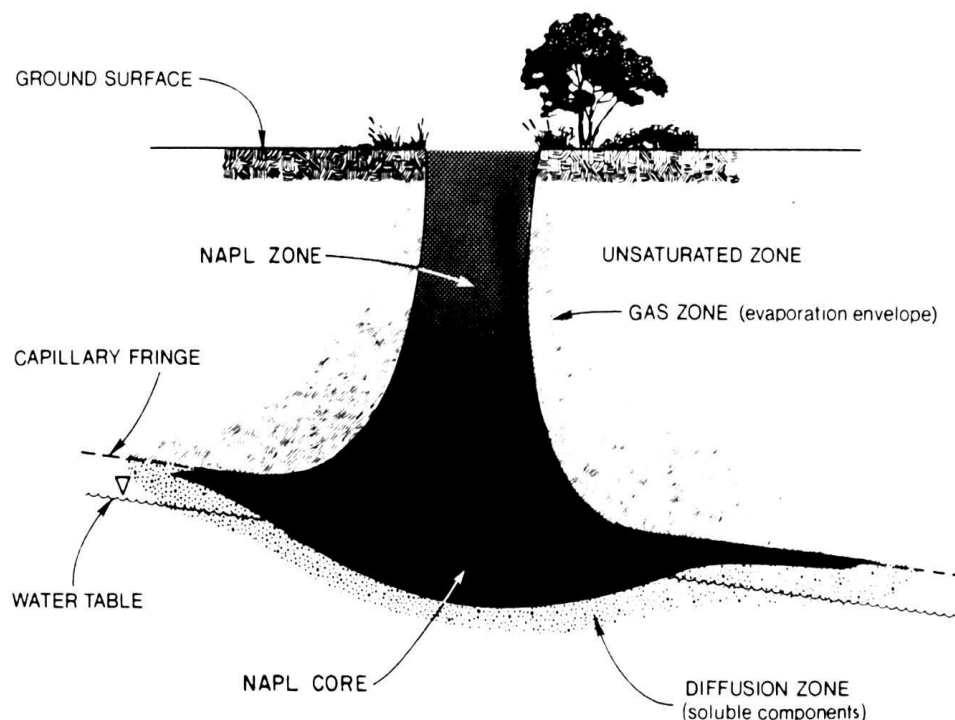


Figure 3.3: Representation of LNAPL movement in the subsurface (modified from Pinder and Abriola 1986)

3.3.1.3 Contaminant Phase Distribution

LNAPL constituents may exist in any of four phases within the subsurface. In the unsaturated zone there are four phases distribution of NAPL, i.e. vapor aqueous, residual and free phase. In the saturated zone contaminants exist in three phase, the residual, aqueous and the free phase. Contaminants may also partition to the solid-phase material (i.e., soil or aquifer materials).

NAPL constituents may partition, or move from one phase to another, depending on environmental conditions. For example, soluble components may dissolve from the NAPL into passing ground water. The same molecule may adsorb onto a solid surface, and subsequently desorb into passing ground water. The tendency for a contaminant to partition from one phase to another may be described by partition coefficients such as Henry's Law constant for partitioning between water and soil gas. These empirical coefficients are dependent on the properties of the subsurface materials and the NAPL. (Huling and Weaver, 1991). It is important to note that this distribution is not static and may vary over time due to remedial actions and natural processes.

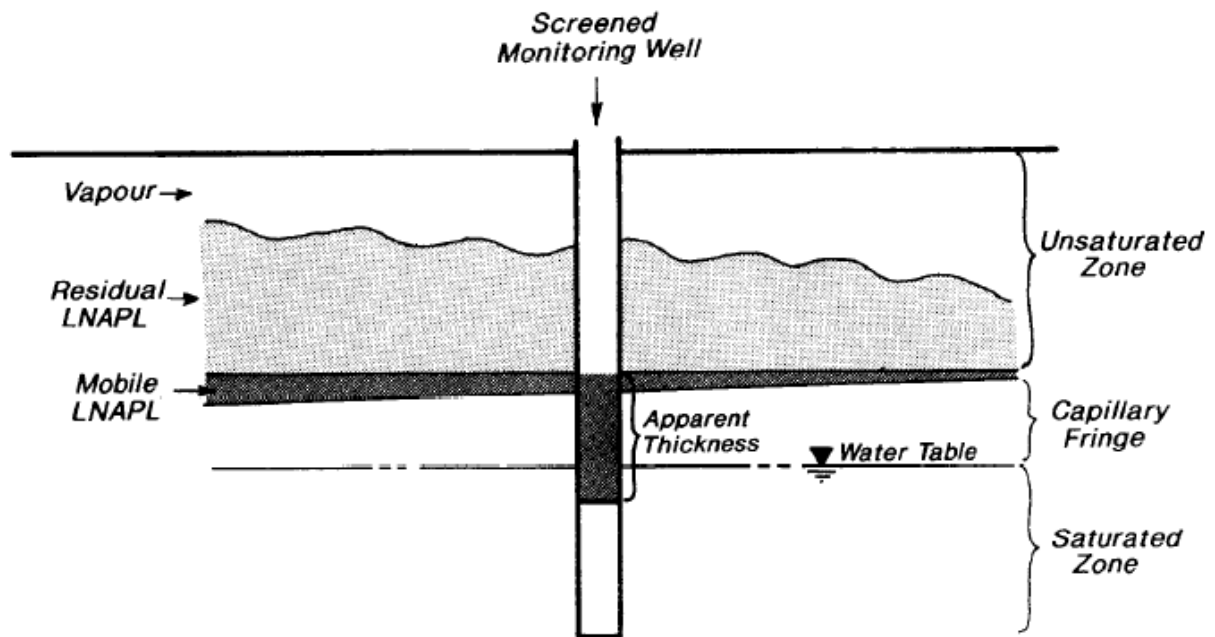


Figure 3.4: Conceptual LNAPL distribution after lateral migration

3.3.1.4 LNAPL transport parameters

LNAPL and subsurface materials are governed with transport parameters at both the pore scale and field scale. At the pore scale, the following transport and fate parameters control LNAPL migration and distribution. At the field scale, LNAPL migration is much more difficult to predict due to such factors as complex release history and, most importantly, subsurface heterogeneity.

3.3.1.4.1 NAPL migration at the pore scale

Multiphase flow processes at the pore scale ultimately controls NAPL movement at the field scale. Therefore an understanding of these processes and the determination of factors affecting flow at this scale provides a foundation for the examination of NAPL migration at larger scales.

3.3.1.4.1.1 Density

The density of a NAPL has a large impact on gravity flow forces. It also determines whether the oil will float or sink if it reaches the water table (Mercer and Cohen 1990). NAPLs lighter than water (LNAPLs) will float and NAPLs denser than water (DNAPLs) will sink in water saturated medium.

3.3.1.4.1.2 Viscosity

Internal fluid resistance to flow is measured by viscosity. Fluids with low viscosities penetrate more rapidly into soil than high viscosity fluids (Mercer and Cohen 1990). If the viscosity of oil is greater than that of water, then the mobility of water is favoured (Mercer and Cohen 1990).

3.3.1.4.1.3 Interfacial tension

At the boundary between immiscible fluids in direct contact there exists a kind of ‘skin’ arising because of the difference between molecular cohesion within a phase and adhesion effects between phases (Schowalter 1979). Interfacial tension is a measure of this difference and influences multiphase flow because of its direct effect on the capillary pressure across the immiscible fluid interface (Mercer and Cohen 1990). The units of interfacial tension are energy per area [*dyne cm⁻¹*].

3.3.1.4.1.4 Wettability

Wettability describes preferential spreading of a fluid onto a solid surface and depends on interfacial tension (Mercer and Cohen 1990). The wetting fluid will tend to spread over grains in preference to the non-wetting fluid. The wetting fluid will occupy smaller voids and pore throats, whereas the nonwetting fluid will be restricted to larger pores (Mercer and Cohen 1990). Wettability can be measured by the contact angle - the angle between the solid surface and the tangent of a drop of the fluid at the solid interface. If the angle between the fluid and the solid interface is less than 90°, the fluid is said to be wetting. If the contact angle is greater than 90°, the fluid is said to be nonwetting (Mercer and Cohen 1990) (Figure below).

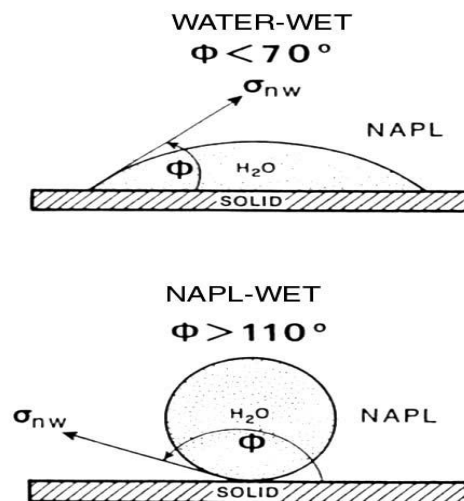


Figure 3.5: Contact angle for wetting and non-wetting fluids. This diagram shows the wettability configurations for water and LNAPL (modified from Mercer and Cohen 1990)

In multiphase systems, water is generally assumed to be the wetting fluid, followed by NAPL then air. This is called the wettability sequence, and is a crucial and common assumption to many multiphase models. However, wettability depends on many factors and so it is spatially variable (Honarpour et al.1986)

3.3.1.4.1.5 Capillary pressure

Capillary pressure is defined as the difference in pressure between the wetting and non-wetting fluid phases in a porous medium (Miller et al. 1998; Mercer and Cohen 1990):

$$P_{CNW} = P_N - P_W \quad (1)$$

where

P_{CNW} : capillary pressure [Pa]

P_N : non-wetting phase pressure [Pa]

P_W : wetting phase pressure [Pa]

Capillary pressure is dependent on interfacial tension, wettability (contact angle) and the pore size distribution of the soil:

$$P_{CNW} = \frac{2\sigma_{NW} \cos\phi}{r} \quad (2)$$

where

r : radius of pore that non-wetting fluid must enter

ϕ : contact angle [degree]

Capillary pressure is a major aspect of multiphase flow as it causes porous media to draw in the wetting fluid and push out non-wetting fluid from smaller pore spaces (Bear 1972) and so affects the shape of a NAPL spill in the unsaturated and saturated zone (Mercer and Cohen 1990).

3.3.1.4.2 NAPL migration at the field scale

The vertical and lateral migration of NAPL in the subsurface at the field scale is controlled by both gravitational and capillary forces (Guarnaccia et al. 1997; Kessler and Rubin 1987; Mercer and Cohen 1990). After release, NAPL flows downward as one continuous phase due to gravity and spreads laterally due to capillary forces, horizontal bedding and spatial variability (Mercer and Cohen 1990; Poulsen and Kueper 1992). Lateral spreading is related to penetration depth because an increase in the horizontal movement of NAPL results in a smaller volume available for penetration (Poulsen and Kueper 1992).

Factors affecting NAPL movement at this scale can be classified into fluid and porous media properties, the nature of NAPL release and subsurface heterogeneity.

3.3.1.4.2.1 Fluid and porous media properties

NAPL migration at the field scale is affected by fluid and porous media properties. These include capillary pressure, saturation and permeability. These three fluid and porous media properties are highly interdependent, or non-linear, because the relative permeability of a fluid depends on its saturation, and saturation depends on capillary pressure. These relationships are called capillary pressure saturation- permeability relations and are a key element of multiphase flow models.

Residual saturation, S_r , is an important aspect of multiphase flow that is related to the capillary pressure-saturation-permeability relationship. After initial subsurface migration, NAPL may become immobilised due to residual liquid becoming entrapped in pore spaces

causing the flow to become discontinuous. The saturation of NAPL when the flow stops is called the residual saturation (Hemond and Fechner 1994):

$$S_r = \frac{V_{NAPL}}{V_{voids}}$$

Values of S_r generally range from 0.10 to 0.30 for mineral oil in sands (Mercer and Cohen 1990).

Residual saturation is controlled by capillary forces (i.e. pore size distribution, interfacial tension, wettability), as well as porosity, intrinsic permeability and initial water saturation, and is therefore highly spatially variable. A large capillary pressure, such as a large NAPL pressure head, increases residual saturation by forcing the non-wetting fluid into smaller pore spaces where it may remain entrapped if pressure is decreased (Mercer and Cohen 1990). Therefore, in the presence of water in the unsaturated zone, NAPL may be retained as residual, or non-wetting blobs (Mercer and Cohen 1990). In the saturated zone, the fluid viscosity ratio, density ratio and hydraulic gradient also control residual saturation. Residual NAPL is difficult to remove or remediate and may cause long term contamination due to slow dissolution or vaporisation.

The displacement entry pressure (P_d) is the capillary pressure that must be overcome for the nonwetting fluid to enter a wetting fluid saturated media (Mercer and Cohen 1990). This principle explains perching of potentially mobile pools of NAPL upon lenses containing soil with a small average pore radius (r). These lenses act as capillary barriers to flow and pathways that require the least capillary resistance to entry are followed

Spill penetration depth is partly controlled by residual saturation. If a greater volume of oil can be held within the pores (residual), then the volume available for further migration is reduced (Poulsen and Kueper 1992). Van Geel and Sykes (1997) illustrated the effects of residual saturation in predicting LNAPL distribution in the unsaturated and saturated zone through numerical modeling and laboratory work.

3.3.1.4.2 Nature of LNAPL released

The nature in which NAPL enters the subsurface has a large effect on the spatial distribution of NAPL migration paths at the field scale (Poulsen and Kueper 1992; Guarnaccia et al. 1997; Feenstra and Cherry 1988). Quite often in real spill scenarios, NAPL release history (in particular volume, duration and infiltration area) is not known, and so investigations into the effects and sensitivity of these parameters are important.

Poulsen and Kueper (1992) examined the effect of source release rate and porous media heterogeneity on the spatial distribution and depth of penetration of tetrachloroethylene (PCE) in the unsaturated zone of a sandy aquifer. They showed that capillary forces dominated the system when the PCE was released as a drip. Under ponded rapid infiltration (“instantaneous”) release, gravity forces only appeared dominant directly beneath the release. The drip release penetrated 1.6 times deeper than the instantaneous release because the cross sectional area was 1000th of the size. Saturation of the NAPL below the instantaneous release was also much larger than for the drip release because the pressure due to ponding could

force the NAPL into smaller pores. The study therefore showed that the depth of penetration was a function of source release strength.

In a similar study, Kueper and Gerhard (1995) investigated the effect of source release location, size and strength (source capillary pressure) on infiltration rates and the degree of lateral spreading of DNAPL into a saturated heterogeneous porous medium. Twenty five numerical simulations in different spatially correlated random hydraulic conductivity fields showed that infiltration rates for point source releases were log-normally distributed with a similar variance to the underlying permeability field. They also showed that lower source capillary pressure releases (i.e. slow, dripping release) of nonwetting liquids results in greater lateral spreading than a catastrophic, high capillary pressure release.

3.3.1.4.2.3 Subsurface heterogeneity

If hydrogeological properties affecting multiphase flow (e.g. permeability, porosity) are spatially variable, then it is intuitive that NAPL distribution in the subsurface will be directly related to this same pattern of heterogeneity.

Past research has explored the response of NAPL migration to variability in subsurface properties. Simulations of Kueper and Frind (1991b) demonstrated the sensitive response of NAPL migration pathways to even relatively minor variations in the capillary properties of the porous medium. They explored the vertical and lateral migration of NAPL in porous media and the encounter with a lens of low permeability. In this case, the NAPL will need to build up the required saturation to create the necessary capillary pressure that will allow the non-wetting fluid to penetrate the lens. Lateral spreading is also promoted above such lenses because of the increases saturation and the dissipation of the pressure head.

Poulsen and Kueper (1992) examined the effect of porous media heterogeneity on the spatial distribution of PCE and also showed that the NAPL migration in sand was sensitive to variations in permeability and capillary characteristics. Kueper and Gerhard (1995) demonstrated that the order of encounter of varying permeability lenses influences the infiltration rate of a non-wetting phase release, and that infiltration rates for equivalent releases in multiple realizations exhibit similar statistical distributions to the fields themselves. Numerical simulations conducted for point source releases also resulted in a lower degree of lateral spreading in an equivalent homogenous medium than the entire ensemble of heterogeneous results. Bradford et al. (1998) generated spatially correlated permeability fields to examine the effect of chemical and physical heterogeneity on DNAPL migration. They found that spatial variations in wettability characteristics can greatly influence aspects of DNAPL distribution such as saturation, lateral spreading and depth of infiltration

4 GPR FOR SOIL CONTAMINATION

4.1 Introduction

Ground penetrating radar (GPR) is a near-surface geophysical technique that can provide high resolution images of the dielectric properties of the top few tens of meters of the earth. Digital radar systems are now available with a range of capabilities and are used for many varied applications including the assessment of groundwater resources, mineral exploration, archaeological studies and environmental applications. Locating and predicting the fate and transport of contaminants in the subsurface requires an accurate model of the physical, chemical, and biological properties of the earth. In applications in contaminant hydrology, radar data can be used to detect the presence of liquid organic contaminants, many of which have dielectric properties distinctly different from those of the other solid and fluid components in the subsurface. The resolution (approximately meter-scale) of the radar imaging method is such that it can also be used in the development of hydrogeologic models of the subsurface, required to predict the fate and transport of contaminants. GPR images are interpreted to obtain models of the large-scale architecture of the subsurface and to assist in estimating hydrogeologic properties such as water content, porosity, and permeability. Its noninvasive capabilities make GPR an attractive alternative to the traditional methods used for subsurface characterization.

GPR can be used to address subsurface contamination problems. The ways in which it can be used is described in terms of three different objectives. The first objective is to use GPR for direct detection to determine the present location of the contaminant. The two other objectives are related to developing an understanding and quantitative model of the long-term transport of the contaminant so as to predict its future location. The second objective can be defined as obtaining a model of the large-scale (meters to tens of meters) geologic structure of the subsurface; this would provide the basic framework required for the development of a hydrogeologic model. The third objective involves assigning values of hydrogeologic properties (e.g. water content, porosity, permeability) within this framework that are needed to accurately model contaminant movement. Regardless of the specific way in which GPR data are used, a critical issue, and an ongoing focus of research, is the development of a fundamental understanding of the relationship between what is seen in the radar image and the true structure and properties of the subsurface of the earth.

4.2 Dielectric properties of geological materials

The dielectric properties of the subsurface are the primary control on both the amplitude and the arrival time of the received energy in a GPR survey. What we image in a GPR survey is thus largely determined by the variation in dielectric properties of the subsurface. If we can image a contaminant with GPR, it is because of a contrast in dielectric properties between the contaminated region and the background “clean” geological materials. If we can determine the hydrogeologic structure or heterogeneity of the subsurface it is because there is a link between the imaged dielectric properties and the hydrogeologic properties of interest. A critical question is, therefore, what controls the dielectric properties of materials in both clean and contaminated regions of the subsurface?

In general, the dielectric permittivity ϵ and the electrical conductivity σ are complex, frequency-dependent parameters that describe the microscopic electromagnetic properties of a material. The former accounts for mechanisms associated with charge polarization, whereas the latter accounts for mechanisms associated with charge transport. Following the sign

convention adopted by Ward & Hohmann (1988), the conductivity and dielectric permittivity are defined as,

$$\sigma(\omega) = \sigma'(\omega) + i\sigma''(\omega)$$

and

$$\varepsilon(\omega) = \varepsilon'(\omega) + i\varepsilon''(\omega),$$

where ω is angular frequency, $\varepsilon'(\omega)$ is the polarization term, $\varepsilon''(\omega)$ represents energy loss due to polarization lag, $\sigma'(\omega)$ refers to ohmic conduction, and $\sigma''(\omega)$ is a faradaic diffusion loss. A detailed discussion of the mechanisms governing these four parameters in Earth materials can be found in Powers (1997) and Olhoeft (1998).

The total response of a material to an oscillating electric field will incorporate all of these mechanisms and can be described either in terms of a total complex permittivity or total complex conductivity. For the purposes of discussing the role of dielectric properties in radar, it is preferable to use the total complex permittivity $\varepsilon_T(\omega)$ given by

$$\varepsilon_T(\varepsilon) = [\varepsilon'(\omega) - i\varepsilon''(\omega)] - \frac{i}{\omega} [\sigma'(\omega) + i\sigma''(\omega)]$$

When the right-hand side of this equation is rearranged, we can form a real part representing the ability of the material to store energy through polarization and an imaginary part representing the ability of the material to transport charge. The resulting real-valued, “effective” permittivity and conductivity are:

$$\varepsilon_{ef}(\varepsilon) = \text{Re}\{\varepsilon_T(\omega)\} = \varepsilon'(\omega) + \frac{\omega\sigma''}{\omega}$$

and

$$\sigma_{ef} = -\omega \text{Im}\{\varepsilon_T(\omega)\} = \sigma'(\omega) + \omega\varepsilon''(\omega).$$

It is commonly assumed that $\sigma''(\omega) = 0$ and that $\sigma'(\omega) = \sigma_{DC}$ the frequency- independent direct current (D.C.) conductivity of the material. For notational simplicity, the (ω) designation will be dropped for the remainder of this review.

The quantity commonly referred to as the dielectric constant, ε , is defined as

$$\varepsilon = \frac{\varepsilon_{ef}}{\varepsilon_0},$$

where ε_0 is the permittivity of free space.

The dielectric properties of a number of contaminants have been measured (along with other useful properties) and are compiled in Lucius et al (1992). There have also been numerous laboratory studies of the dielectric properties of various rocks, sediments, and solids, to determine how ε of the total system (solids and fluids) is affected by frequency of measurement and various material properties such as composition, porosity, water content, and microgeometry. Some of these laboratory studies, relevant to environmental applications of GPR where measurements were made in the frequency range of 1Mz to 1GHz, are summarized in Table 4.1 (which is a modified version of Table 4.1 in Knoll 1996).

Table 4.1: Experimental investigations of the dielectric properties of geological materials

Reference	Frequency Range	Material	Physical properties
Smith-Rose 1933	100 kHz–10 MHz	Natural soils	Water content
Keller & Licastro 1959	50 Hz–30 MHz	Rocks	Water content
Scott et al 1967	100 Hz–1 MHz	Natural soils, rocks	Water content
Lundien 1971	10 MHz–1.5 GHz	Natural soils	Water content, bulk density, lithology
Birchak et al 1974	4 GHz–6 GHz	Clay, crushed Limestone	Water content
Hipp 1974	30 MHz–4 GHz	Natural soils	Water content, bulk density
Hoekstra & Delaney 1974	100 MHz–26 GHz	Natural soils	Water content
Poley et al 1978	1.5 kHz–2.4 GHz	Sandstones, carbonates	Lithology, porosity, water Saturation
Hall & Rose 1978	200 Hz–1 GHz	Clays	Water saturation, clay microstructure
Okrasinski et al 1979	390 MHz–1.5 GHz	Natural soils	Water content, porosity
Topp et al 1980	20 MHz–1 GHz	Glass beads, natural Soils	Water content
Wang & Schmutge 1980	1.4 GHz–5 GHz	Natural soils	Water content, clay content
Sen et al 1981	1.1 GHz	Sintered glass beads	Porosity, geometry, pore fluid content
Lange 1983	100 MHz–1 GHz	Glass beads, natural soils	Porosity, surface area/pore volume, saturation
Kenyon 1984	500 kHz–1.3 GHz	Carbonates	Water-filled porosity, grain geometry
Hallikainen et al 1985	1.4 GHz–18 GHz	Natural soils	Water content, clay content
Shen et al 1985	800 MHz–1.2 GHz	Sedimentary rocks	Water-filled porosity

4.3 Detecting contaminants with radar data

In contaminant hydrology, GPR is mostly used for the direct detection of a contaminant. This project focuses on contaminant detection with GPR which will address the specific issue of detection of immiscible liquid-phase organics, which has been a major focus within the geophysical community.

The ability of GPR to detect a contaminant requires that the presence of the contaminant perturbs the dielectric properties of the subsurface sufficiently to result in a detectable change with the GPR measurement. The dielectric constants of the top 10 organic contaminants, listed with respect to frequency of occurrence range from approximately 2 to 10 (Lucius et al 1992).

Table 4.2: Top 10 organic chemical contaminants by frequency of occurrence (Plumb and Pitchford, 1985) along with selected physical properties (from Lucius and others, 1990).

Chemical	CASRN	SG	sol	vap	ϵ	Log R	Electro	clay
Trichloroethane(TCE)	79-01-6	1.46	0.11	8	3.42	6	?	yes
Dichloromethane	75-09-2	1.32	1.5	50	8.93	8	Yes	?
Tetrachloroethane(PCE)	127-18-4	1.6	0.01	2	2.28	7	?	yes
Toluene	108-88-3	0.87	0.05	4	2.4	7	Yes	yes
1,1- Dichloroethane	75-34-3	1.17	0.5	10	?	7	25	?
Bis(2-ethylhexyl)phthalate	117-81-7	0.89	4e-5	1e-5	5	?	?	?
Benzene	71-43-2	0.879	0.17	10	2.28	9	Yes	yes
trans-1,2-Dichloroethene	165-60-5	1.26	0.6	40	2.1	?	?	yes
1,1,1-Trichloroethane	71-55-6	1.33	0.2	14	7.5	6	?	yes
Chloroform	67-66-3	1.49	0.8	4.8	20	8	Yes	yes

CAS RN is Chemical Abstracts Service Register Number (the most unambiguous label for a chemical). **SG** is specific gravity in g/cm³. **sol** is aqueous solubility in weight percent. **vap** is the vapor pressure in kiloPascals. **ϵ** is dielectric permittivity relative to free space. **logR** is the electrical resistivity in log₁₀ ohm-m. **electro** and **clay** indicate whether or not anything is known about the electrochemical or clay-organic reactivity of that chemical respectively. All property values are shown to most significant known digit near 20°C.

For example, the first three on this list are trichloroethylene (TCE), $\epsilon = 3.42$ (measured at 10°C); dichloromethane $\epsilon = 8.93$ (measured at 25°C); and tetrachloroethylene or perchloroethylene (PCE), $\epsilon = 2.28$ (measured at 25°C). Given the contrast between these values of ϵ for an organic contaminant and that of water ($\epsilon = 80$), it is clear that if a contaminant displaces water in a region of the subsurface; there will be a distinct change in the dielectric constant of that region.

The first well-known controlled field experiment conducted specifically to assess the use of GPR for the detection of organic contaminants was the work performed in 1991 at the Borden field site by the University of Waterloo and described in a series of publications (Greenhouse et al 1993, Brewster & Annan 1994, Sander 1994, Brewster et al 1995). A total of 770 L of PCE was introduced through an injection well into a sand-filled cell, $9m \times 9m \times 3m$ deep. Injection occurred over a period of 70 hours with GPR data collected at regular intervals up to 340 hours after the start of the spill. The GPR images of PCE, which is denser than water, sinking through water-saturated sand provided convincing evidence that monitoring of contaminant movement with radar data is in fact possible.

4.4 Undetectable organics

The mapping of contaminants of some organics such as bis (2-ethylhexyl) phthalate by noninvasive geophysical methods is impossible. This is because the physical properties of these undetectable organics do not contrast with the geologic media within which they reside. Similarly, highly water soluble organics, such as alcohols, are inherently undetectable to noninvasive geophysical methods. Only chemical sampling or borehole measurements can detect these organic contaminants. All organic chemical contaminants are undetectable by noninvasive geophysical methods at the typical concentration (ppm or ppb) levels of regulatory concern. At such levels, the presence of the contaminant and its location may only be inferred from the geophysical mapping of geological structure and migration pathways, or

through observations of subtle changes in geohydrological heterogeneity and geological background statistics (Olhoeft, 1991).

4.5 LNAPL detection and mapping with GPR

The misuse, spillage and uncontrolled disposal of Light Non-Aqueous Phase Liquid (LNAPL) contaminants such as petroleum fuels, solvents, coal-tars and other mobile hydrocarbons poses serious groundwater, land and public health problems throughout the industrialised and developing world. As many LNAPLs are both sparingly soluble and highly mobile, assessing their time-varying concentrations and sub-surface distribution can be extremely difficult, particularly in complex, near-surface industrial environments. Traditionally, expensive programs of site investigation, distribution modeling, excavation, drilling and sampling are required in order to determine the exact nature of any contamination event. However, in the past decade non-invasive geophysical investigation techniques have become increasingly prevalent with 'geo-electrical' methods such as electrical resistivity, induced polarisation (IP), electromagnetic conductivity (EM) and, more specifically, Ground Penetrating Radar (GPR) becoming increasingly popular (e.g., [Olhoeft, 1992], [Benson and Stubben, 1995], [Daniels et al., 1995], [Sauck et al., 1998], [Atekwana et al., 2002], [Osella et al., 2002], [Burton et al., 2004], [Sogade et al., 2006] and [Abdel Aal et al., 2006]). Although these, plus many other cases, have shown that geophysical methods can be used to successfully image LNAPL contaminants, there is still a debate on the interpretation of the observed results. Initially, LNAPL contamination was associated with high electrical resistivities, low conductivities and reduced levels of GPR signal attenuation, as observed in controlled spill and short-term laboratory experiments ([DeRyck et al., 1993] and [Lien and Enfield, 1998]). This was based on the notion that the relatively high resistivity NAPL components would produce an insulating layer around the matrix grains, therefore, reducing the bulk electrical conductivity of the materials (Mazác et al., 1990). However, a large volume of recent research has shown that aged or mature LNAPL spills undergo a significant process of alteration and biodegradation that actually increases the bulk conductivity of the LNAPL contaminated zone. This is particularly true where the LNAPL is in a free-phase form and associated with saturated ground waters in anaerobic conditions ([Baedecker and Cozzarelli, 1994], [Cozzarelli et al., 1994] and [Cozzarelli et al., 2001]). These observations has been supported by in-situ investigations, laboratory experiments ([Cassidy et al., 2001], [Acworth, 2001], [Atekwana et al., 2004a], [Atekwana et al., 2004b] and [Atekwana et al., 2004c]) and through the analysis of surface conductivity, resistivity and GPR signal attenuation/reflection studies ([Kim et al., 2000], [Sneedon et al., 2000], [Atekwana et al., 2000], [Atekwana et al., 2002], [Osella et al., 2002] and [Bradford, 2003]). In general, it would appear that the process of physical/chemical alteration of the hydrocarbon contaminants by natural micro-organisms is responsible for generating elevated levels of biosurfactants plus mobile organic and carbonic acids. These acids are then responsible for the accelerated dissolution of feldspars and quartz in the matrix materials ([Cozzarelli et al., 1994], [McMahon et al., 1995], [Cozzarelli et al., 2001], [Cassidy et al., 2001] and [Abdel Aal et al., 2006]) and, as a result, the dissolved ions, organic acids and dispersed bacteria enter the pore and groundwaters increasing the electrical conductivity and, therefore, reducing the bulk resistivity. Although this mechanism is reasonably well understood and documented, there is still some ambiguity in the geo-electrical results at many of the investigated LNAPL sites. Reports of enhanced bulk electrical resistivity (and, therefore, reduced electrical conductivity) have conflicted with the observations of reduced resistivities at comparable sites (Atekwana et al., 2000). Similarly, GPR data from a number of sites appears to suggest that the presence of high-conductivity, LNAPL degradation products results in the preferential attenuation of the GPR signal and the presence of 'shadow zones' in

the GPR sections ([Atekwana et al., 2000] and [Atekwana et al., 2002]). Investigations have also shown that LNAPL products can produce increased amplitude reflections, or 'bright-spots', in the GPR sections that are usually associated with the sharp interfaces created at the boundary between the high-permittivity, low-resistivity ground waters and the low-permittivity, high-resistivity, LNAPL saturated, materials (e.g., [Benson, 1995] and [Campbell et al., 1996]). Conversely, it is also possible to observe 'dim spots' in the reflection response from the groundwater interface where isolated or thin zones of free-phase LNAPLs are preferentially attenuating/scattering the GPR signal.

Ultimately, all interpretations are valid as the physical/hydrological complexity of the sub-surface environment, the contaminant history and the nature of the original spill conditions dictates how a site will respond to a particular geophysical survey. From experience, it is common to find a range of GPR responses at any given LNAPL contaminated site with shadow zones being co-incident with 'bright spot' reflections and signal attenuation varying significantly over the site. This level of complexity is becoming more evident in recent, practical LNAPL-related GPR papers, (e.g., Lopes de Castro and Branco, 2003) as our understanding of the physical evolution of a LNAPL spills moves away from the simple, four-component vapour, residual, free and dissolved phase model to a more complex, mixed-component, multi-phase 'smeared zone' model associated with temporal changes in the depth of the groundwater horizon (Lowe et al., 1999). In this scenario, it is possible for mobile LNAPL products to preferentially follow the higher-permeability pathways created by variations in pore space rather than the localised hydraulic gradient (Lowe et al., 1999). Consequently, transportation pathways and, therefore, contaminant distribution is likely to be governed by the nature of the sub-surface structures rather than the natural flow of the groundwaters. This results in the LNAPLs being 'smeared' across the sub-surface in disaggregated units that, depending on the contaminant's viscosity and localized capillary pressure, may become immobile under unconfined conditions. Because of this complexity, it is not surprising that the LNAPL related GPR surveys have tended to focus on contaminant plume identification only, with less effort being applied to developing more advanced investigation techniques that can 'extract' the hydrological information from the GPR data. Nevertheless, studies by Marcak and Golebiowski (2006), Lopes de Castro and Branco (2003), (Carcione et al., 2006), (Carcione et al., 2003) and (Carcione et al., 2000) and Carcione and Seriani (2000) have shown that, through the judicious use of numerical modeling and/or advanced data processing (such as attribute analysis methods) it is possible to obtain important information on the nature of a particular contaminant problem and its evolution through time (e.g., estimates of volumetric LNAPL saturation, contaminant distribution and the presence/absence of significant migration pathways, etc.). However, before these 'advanced interpretational methods' are accepted by the general hydrological and environmental community, their practical suitability and limitations must be fully evaluated under 'real' site conditions. Therefore, this research aims to be a novel 'case study' into the practical application of GPR-based, attenuation analysis methods in combination with laboratory-based, dielectric material testing technologies. As part of larger programme of investigation utilising other geophysical methods (such as electrical resistivity), the work builds on the findings of (Cassidy, 2004) and (Cassidy, 2006) and has the overall objective of addressing some of the key interpretational issues associated with LNAPL contaminated environments.

In particular, from the signal attenuation characteristics alone, can GPR be used to differentiate between the 'clean' and contaminated areas of the site and/or the unsaturated, smeared and groundwater saturated zones?

At what level of LNAPL saturation does the GPR attenuation become identifiable using signal analysis techniques (such as attribute analysis, etc.)?

What influence does the nature of the LNAPL contaminant have on the GPR signal attenuation (i.e., the presence/absence of free-phase, residual or dissolved phases)?

What is the dominant GPR signal attenuation mechanism occurring in the subsurface (e.g., ionic conductivity losses, scattering/clutter losses, etc.) and can it be related to any specific physical/hydrological feature or bio-chemical process?

Is the nature of the GPR signal attenuation consistent with other measured geophysical characteristics (i.e., the bulk resistivity/conductivity properties determined from electrical resistivity surveys)?

Ultimately, these objectives form part of the general goal of producing realistic signal attenuation models for the improved interpretation of LNAPL-based GPR data and, as such, will provide investigators with practical insights into the merits and limitations of GPR-based analysis studies for other LNAPL contaminated sites.

5 Case Studies of Contaminant Detection with GPR

This section discusses case histories of contaminated site. Ground penetrating radar as non-destructive geophysical technique was used to detect, locate and map the extent of contaminated plumes.

5.1 Canadian Force Base Borden

On April 8, 1999, 50 litres of a dense non-aqueous phase liquid were released into a natural groundwater flow field at Canadian Force Base Borden. The experiment site was conducted in the unconfined aquifer at Canadian Force Base Borden which is located approximately 90 km northwest of Toronto, Ontario, Canada. The Borden test site is consists of fine to medium sand aquifer underlined by medium stiff clay aquitard. The water table depth seasonally varies between 0.5 and 1.5 m below the ground surface at the test site location. The experiment was performed in a 4.2 m × 4.25 m area (Figure 1). There were 18 profile lines. Ground penetration radar profiling with 200 MHz antennas was conducted before and after the release until the Fall 2004 to detect the location of the immiscible solvent pools and monitor their evolution with time.

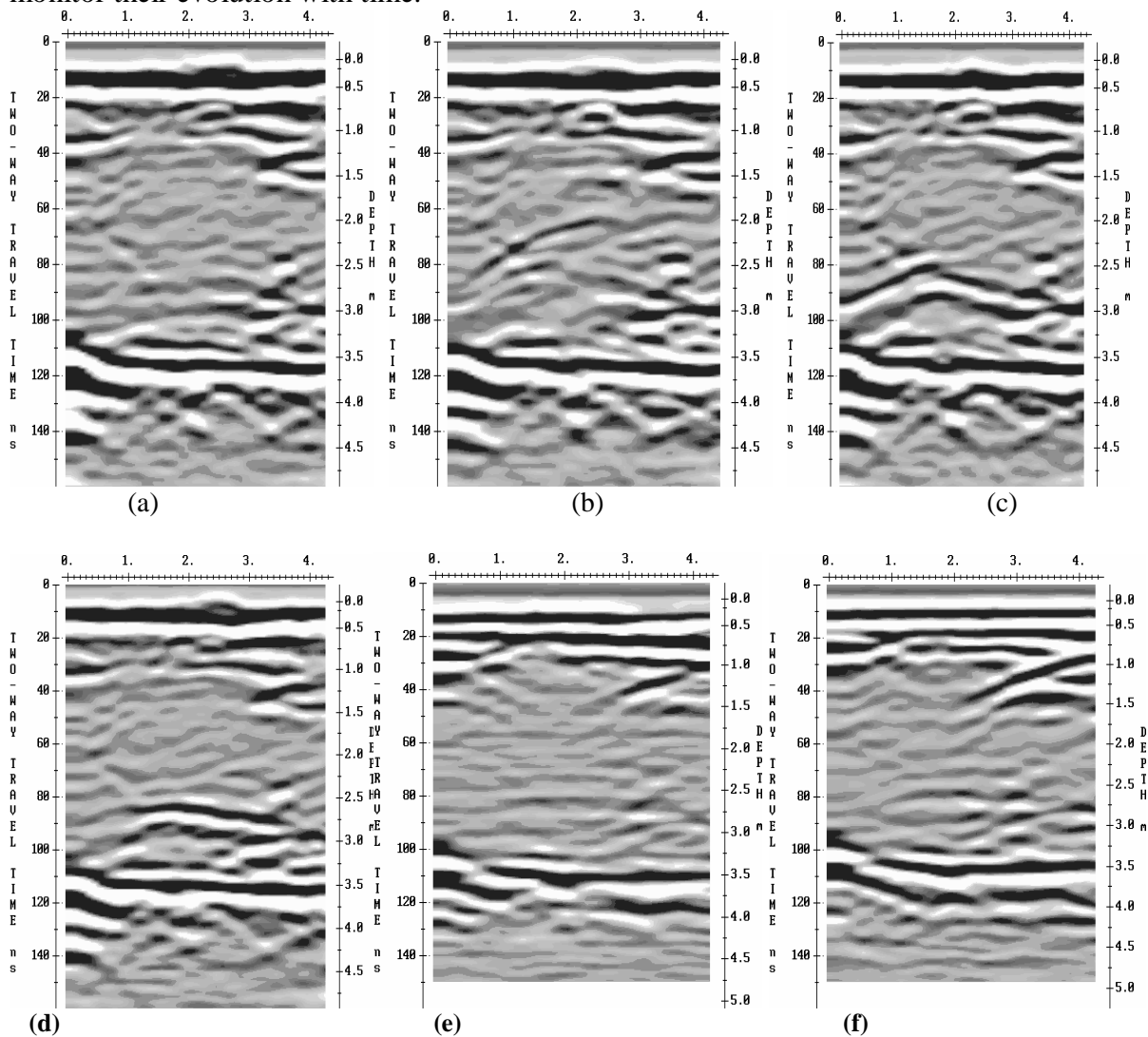


Figure 5.1: GPR profiles along one of the survey Lines: (a) before the injection; (b) 1/2 day after; (c) one day after; (d) two weeks after; (e) two years after; (f) five years after. Position axis units are meters; time axis units are nanoseconds.

Even though the volume of DNAPL injection was relatively small (50 litres), GPR profiling detected significant changes in reflectivity from which the location of solvent pools was inferred and their evolution over time in a natural groundwater flow field. The development of DNAPL pools on the stratigraphic boundaries as a result of downward migration and accumulation of the solvent was clearly seen on the early time GPR profiles (1/2 day - 2 weeks after the injection). The long-term evolution of the DNAPL was observed on the late time GPR profiles (two and five years after the injection). During this period, there was a reduction and the almost complete dissipation of the reflections associated with these pools (Yong Keun Hwang et al Anon)

5.2 Naval Air Station

GPR survey together with other geophysical methods was performed at Naval Air Station, Brunswick, Maine to provide a better understanding of the possible migration pathways of the contaminants in bedrock fractures and deeper stratigraphic zones whose geometries might be controlled by bedrock morphology. The Eastern Plume at Naval Air Station (NAS) Brunswick, Maine, has been attributed to past solvent disposal practices producing groundwater contamination from chlorinated volatile organic compounds (VOCs). The former Fire Department Training Area was one of three primary source areas for the plume. Training activities at this site covering almost 4 decades resulted in significant introduction of VOCs into the groundwater. The area provided recharge to shallow and deep overburden aquifers and also provided recharge to the bedrock aquifer. A plume of the VOC-impacted groundwater extends in the deep overburden aquifer along the eastern boundary of the base, which is on the United States Environmental Protection Agency's (US EPA) National Priorities List. The primary objectives were to map the bedrock surface, ground-truth photo-lineaments, and identify other possible fracture zones that might serve as contaminant pathways. Secondary objectives included mapping key stratigraphic horizons, specifically the Presumpscot Clay, interpreted as the natural barrier to both vertical and lateral migration of the plume.

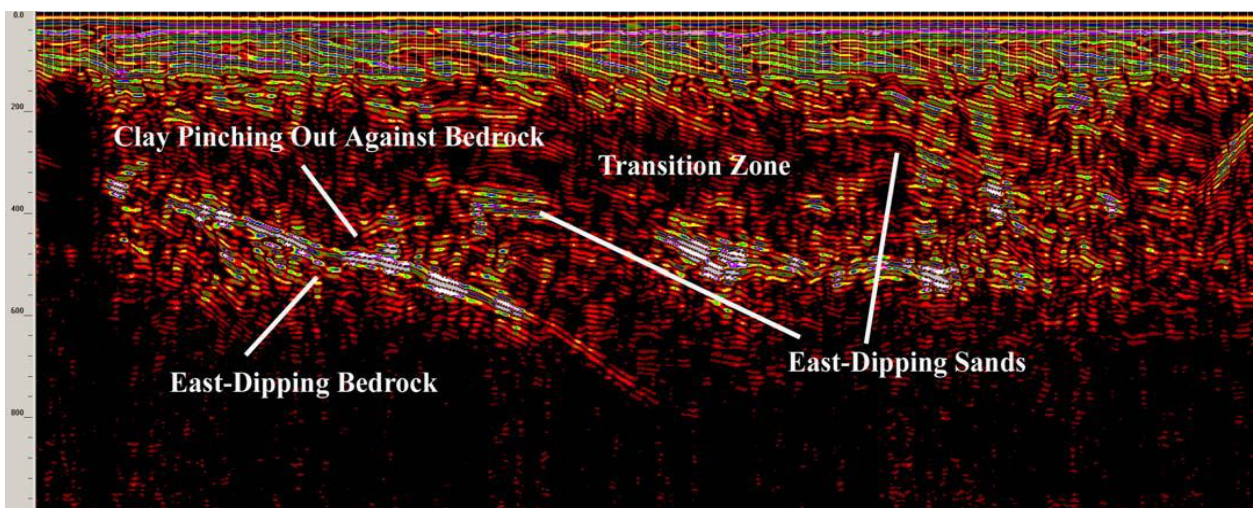


Figure 5.2: A portion of the record for one of the GPR Lines showing east-dipping sands and bedrock, as well as clay pinching out against the bedrock (near bedrock “notch”).

Geophysical data were combined with existing borehole and cone penetrometer information to produce an integrated database that was used to create models of the bedrock and key stratigraphic surfaces. The geophysical investigations and stratigraphic modeling showed the

geological constraints on migration of the Eastern Plume at Naval Air Station, Brunswick (Mario Carnevale et al Anon).

5.3 Brazil

A multifrequency GPR was used for contaminated site mapping together with Electrical Resistivity geophysical methods at a Brazilian site. The area presented hydrocarbon contamination with LNAPL substances on a fuel supply and maintenance areas of train engines and vehicles over operating railroads. The main source of the hydrocarbon contamination was attributed to the fuel activities that had been going on. The spreading of the contaminants in the subsurface on a very porous layer had been linked to the ground water flow. A GPR survey was conducted over this area with an RIS 2K from IDS Italy, with 200 and 600 MHz antennas. Investigation lines were positioned every 2 meter and the depth ranged from 0.6 meters to 3.6 meters below the subsurface. Some anomalies were detected under the fuel supply soil pavement. The results showed a higher electromagnetic attenuation at the area just below the fuel supply concrete pavement and this was detected and mapped with the GPR (Debora Silveira Carvalho et al Anon).

5.4 FT-2-plume at the Wurtsmith Air Force Base

The Fire Training Cell (FT-02) is part of the decommissioned Wurtsmith Air Force Base in Oscoda Michigan. The geology of the site consisted of coarsening downward fine to medium grained eolian sand deposits approximately 20m thick. In cores the water table usually coincided with a thin gravel layer at 3-5m in depth. There was a 6-30m thick silty clay layer below the sands which was believed to be confining the contaminants to the sediments above it.

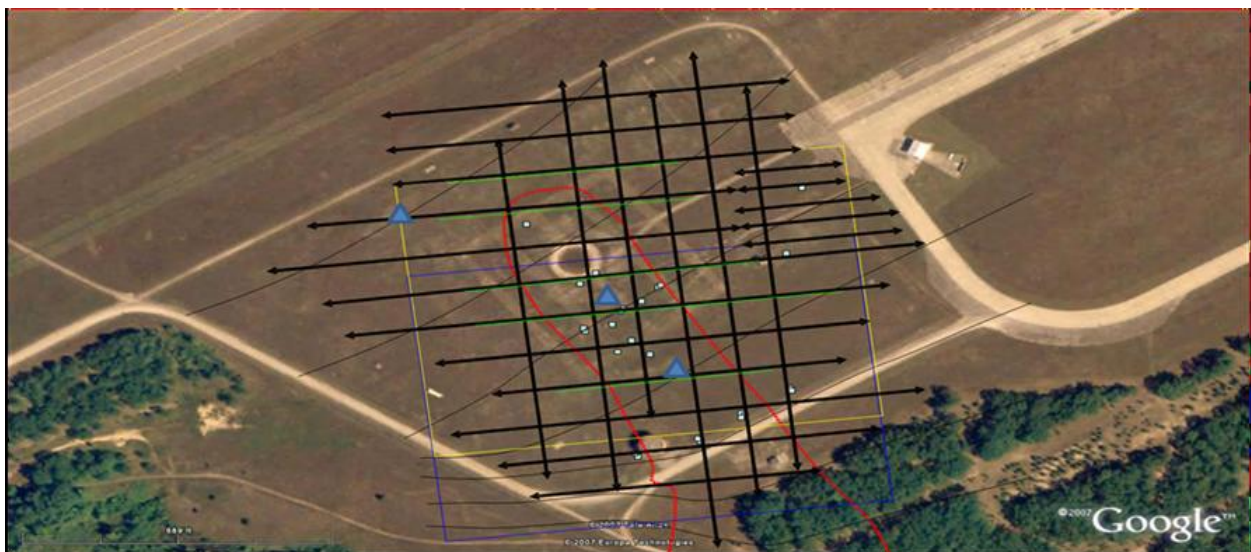


Figure 5.3: Google Earth image overlain by our field grid (black lines). Red line is the plume outline.

This site was used by the Air Force for their bi-weekly exercises where several thousand gallons of left over jet fuel and solvents were dumped onto an old car or airplane body and ignited it. These exercises were conducted from 1952 through 1986 and over time the unburned hydrocarbons seeped through the ground and encountered the water table below. There was a downward migration along the gradient after the contaminants reached the water table. A concrete pad was installed in 1982 by the Air force over the site to prevent further contamination. Groundwater geochemistry studies defined a contaminant plume that was approximately 125 m wide and > 300 m long. Previous GPR surveys had been conducted over the area. The investigations revealed that there were prominent attenuation of the GPR signals by the

contaminant mass just above the water table. Later, researchers in 2007 returned to the site expecting to image a largely unchanged plume but they found out from the GPR data that the plume had significantly reduced in size. The GPR data shows a progressive downward migration of the contaminant mass over time. This was due to the some remediation systems that had been installed over the site (R. Joyce et al)

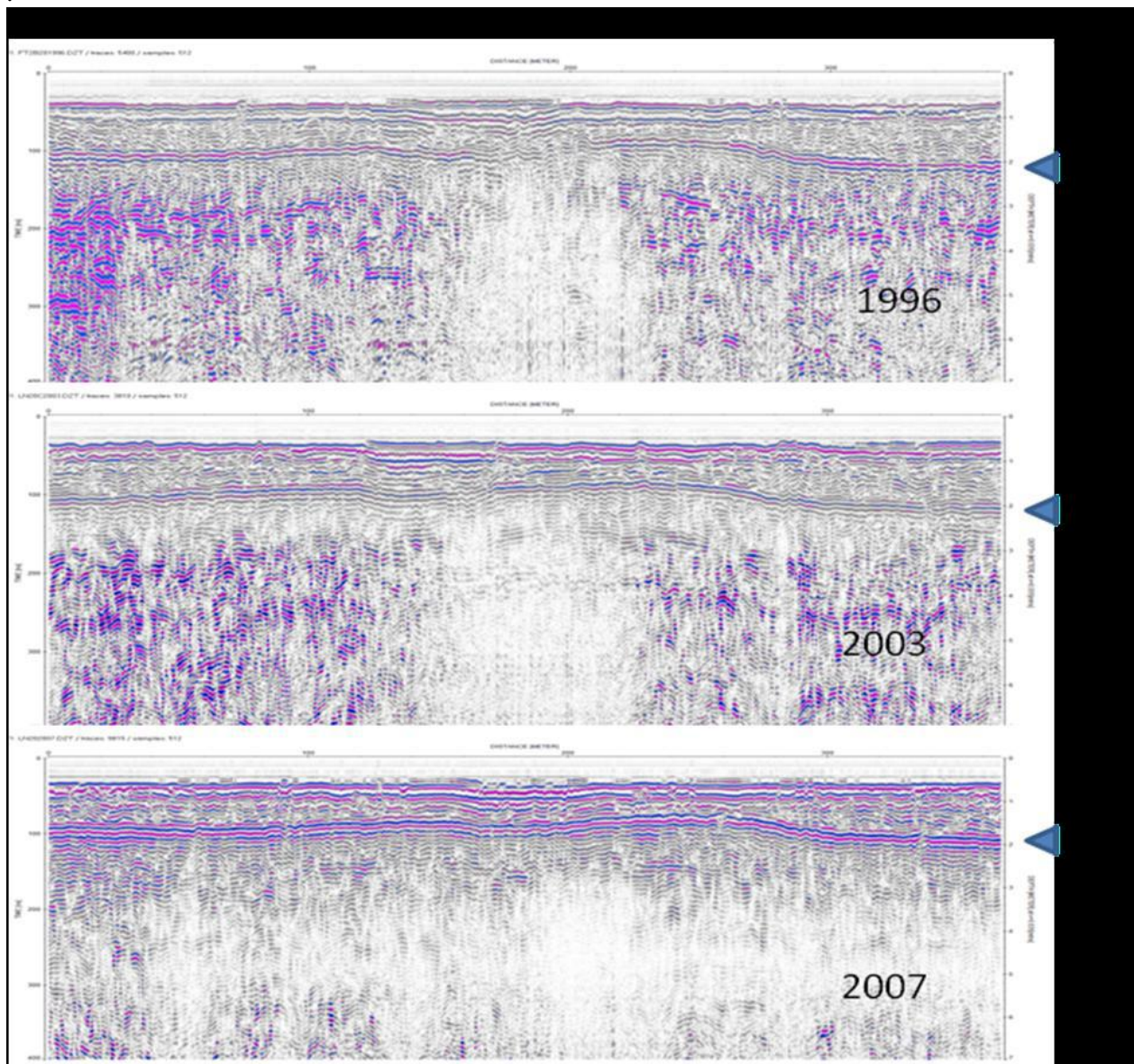


Figure 5.4: GPR profiles across one of the lines showing the decrease in contaminant mass over time.

6 Conclusions and Recommendations

Ground penetrating radar is a high resolution geophysical technique that can remarkably provide images of the subsurface of the earth. A GPR image corresponds to the interaction between electromagnetic waves and the dielectric properties of the subsurface. The images obtained contain a great deal of information. These images can be transformed into quantitative images of the relevant properties of the subsurface. The various limitations with the traditional methods of subsurface characterization have led to the tremendous need of non-invasive technologies for acquiring qualitative information about contaminants in the subsurface. Besides the advantage of the GPR being a non-destructive technique, there are a lot of benefits which include the ability of locating the position and degree of contaminant plumes very quickly and economically. As a result of this, the implementation of this technique as a preliminary tool for remediation strategies of contaminated plumes is highly encouraged.

The wide range of improvements with regards to this technique cannot be left out. Data acquisition, processing and inversion as well as data interpretation have significantly improved. Various GPR brands have conducted in - depth research on GPR and this has resulted in the production of more modern and sophisticated types to meet the challenges of the geophysical field today. These brands have post processing software which is compatible with modern and latest version of operating systems-windows 7. In the past, GPR systems were made up of individual components that the operator had to assemble and interconnect. Now, there are complete GPR systems crafted into a single package providing high performance and ease-of-use. Some also have GPS supports that provide accurate positioning when surveying. Modern GPR's have technologies for networking together any number of GPR units to create virtually any multi-channel GPR deployment imaginable. Gone were the days when data acquisition needed to be done on the field and processing of data done at the office. Investigation with the GPR can be done in real time mode.

Moreover, the GPR works well when applied in profiling shallow contaminated plumes or other anomalies in the subsurface. In addition to, a general idea about the area to be investigated and skilled personnel are needed when GPR is to be used.

Based on the various case studies discussed in our work, there is no doubt that GPR can be used for the location and mapping of contaminant plumes.

It was part of the initial plan of this thesis to use the GPR to locate and map out contaminant plumes in a contaminated site but due to time constraints and reasons beyond our control, we were not able to achieve this objective. As a result, we would like to recommend this to future students who would love to continue from where we reached.

REFERENCES

A. Osella, M. de la Vega and E. Lascano, Characterisation of a contaminant plume due to a hydrocarbon spill using geoelectrical methods, *Journal of Environmental and Engineering Geophysics* 7 (2) (2002), pp. 78–87.

A.K. Benson, Applications of ground penetrating radar in assessing some geological hazards: examples of groundwater contamination, faults, cavities, *Journal of Applied Geophysics* 33 (1995), pp. 177–195.

Abriola, L.M. and Pinder, G.F. 1985a, A multiphase approach to the modeling of porous media contamination by organic compounds, 1. Equation development, *Water Resources Research*, 21(1):11-18.

Abriola, L.M. and Pinder, G.F. 1985b, A multiphase approach to the modeling of porous media contamination by organic compounds, 2. Numerical simulation, *Water Resources Research*, 21(1): 19- 26.

B.K. Lien and C.G. Enfield, Delineation of subsurface hydrocarbon contaminated distribution using a direct push resistivity method, *Journal of Environmental and Engineering Geophysics* 2–3 (1998), pp. 173–179.

B.L. Burton, G.R. Olhoeft and M.H. Powers, Frequency spectral analysis of GPR data over a crude oil spill, *Proceedings of the Tenth International Conference on Ground Penetrating Radar*, Delft, The Netherlands (2004), pp. 267–270

Benson and Stubben, 1995 A.K. Benson and M.A. Stubben, Interval resistivities and very low frequency electromagnetic induction — an aid to detecting groundwater contamination in space and time: a case study, *Environmental Geosciences* 2 (1995), pp. 74–84.

Bradford, S.A., Abriola, L.M. and Rathfelder, K.M. 1998, Flow and entrapment of dense nonaqueous phase liquids in physically and chemically heterogeneous aquifer formations, *Advances in Water Resources*, 22(2): 117-132.

Brewster ML, Annan AP, Greenhouse JP, Kueper BH, Olhoeft GR, et al. 1995. Observed migration of a controlled DNAPL release by geophysical methods. *GroundWater* 33:977–87

Brewster ML, Annan AP. 1994. Ground penetrating radar monitoring of a controlled DNAPL release. *Geophysics* 59:1211–21

C. Kim, J.J. Daniels, E.D. Guy, S.J. Radzevicius and J. Holt, Residual hydrocarbons in a water-saturated medium: a detection strategy using ground penetrating radar, *Environmental Geosciences* 7 (4) (2000), pp. 169–176.

Charles J. Newell, Steven D Acree, Randall R. Ross and Scott G. Huling , EPA ground water issue(Albertis lectural notes)

Conyers, Lawrence B., and Dean Goodman.1997. *Ground-Penetrating Radar: An Introduction for Archeologists*. Walnut Creek, Cal.: AltaMira Press.

D. Lopes de Castro and R.M.G.C. Branco, 4-D ground penetrating radar monitoring of a hydrocarbon leakage site in Fortaleza (Brazil) during its remediation process: a case history, *Journal of Applied Physics* 54 (2003), pp. 127–144.

D.F. Lowe, O.L. Carrol and C.H. Ward, Editors, *Surfactants and Cosolvents for NAPL Remediation, A Technologies Practice Manual*, Lewis Publishers, London (1999).

D.L. Campbell, J.E. Lucius, K.J. Ellefsen and M. Deszcz-Pan, Monitoring of a controlled LNAPL spill using ground penetrating radar, *Proceedings of the Symposium on the Application of Geophysics to Engineering and Environmental Problems (SAGEEP)*, Keystone CO (1996), pp. 511–517.

D.P. Cassidy, D.D. Werkema, W.A. Sauck, E.A. Atekwana, S. Rossbach and J. Duris, The effects of LNAPL biodegradation products on electrical conductivity measurements, *Journal of Environmental and Engineering Geophysics* 6 (1) (2001), pp. 47–53.

D.P. Cassidy, D.D. Werkema, W.A. Sauck, E.A. Atekwana, S. Rossbach and J. Duris, The effects of LNAPL biodegradation products on electrical conductivity measurements, *Journal of Environmental and Engineering Geophysics* 6 (1) (2001), pp. 47–53.

Debora Silveira Carvalho and Roberto Okabe. 2006. Contaminated site mapping using GPR and Electrical Resistivity in Brazil.

E.A. Atekwana, D.D. Werkema Jr., J.W. Duris, S. Rossbach, E.A. Atekwana, W.A. Sauck, D.P. Cassidy, J. Means and F.D. Legall, In-situ apparent conductivity measurements and microbial population distribution at a hydrocarbon contaminated site, *Geophysics* 69 (1) (2004), pp. 56–63.

E.A. Atekwana, E.A. Atekwana, F.D. Legall and R.V. Krishnamurthy, Field evidence for the detection of microbial activity, *Geophysical Research Letters* 31 (2004), p. L23603.

E.A. Atekwana, E.A. Atekwana, R.S. Rowe, D.D. Werkema and F.D. Legall, Total dissolved solids in ground water and its relationship to bulk conductivity of soils contaminated with hydrocarbons, *Journal of Applied Geophysics* 56 (2004), pp. 281–294.

E.A. Atekwana, W.A. Sauck and D.D. Werkema, Investigations of geoelectrical signatures at hydrocarbon site, *Journal of Applied Geophysics* 44(2000), pp. 167–180.

E.A. Atekwana, W.A. Sauck, G.Z.A. Aal and D.D. Werkema Jr., Geophysical investigations of Vadose Zone conductivity anomalies at a hydrocarbon contaminated site: implications for the assessment of intrinsic bioremediation, *Journal of Environmental and Engineering Geophysics* 7 (3) (2002), pp. 103–110.

Feenstra, S. and Cherry, J.A. 1988, Subsurface contamination by dense non-aqueous phase liquids (DNAPL) chemicals, Paper presented at the International Groundwater Symposium, International Association of Hydrogeology, Halifax.

G.Z. Abdel Aal, L. Slater and E.A. Atekwana, Induced-polarisation measurements on unconsolidated sediments from a site of active hydrocarbon biodegradation, *Geophysics* 71 (2) (2006), pp. H13–H24

- GeoRadar Inc. <http://www.geo-radar.pl/en/methods/georadar/working/>
- Greenhouse J, Brewster M, Schneider G, Redman D, Annan P, et al. 1993. Geophysics and solvents: the Borden experiment. *Lead. Edge* 12:261–67.
- Guarnaccia, J., Pinder, P. and Fishman, M. 1997, NAPL: Simulator Documentation, United States Environmental Protection Agency, USA.
- Guarnaccia, J., Pinder, P. and Fishman, M. 1997, NAPL: Simulator Documentation, United States Environmental Protection Agency, USA.
- H. Marcak and T. Golebiowski, A stochastic interpretation of GPR data concerning the location of hydrocarbon plumes, *Near Surface Geophysics* 4 (3) (2006), pp. 163–176.
- Hemond, H. and Fechner, E. 1994, *Chemical Fate and Transport in the Environment*, Academic Press, San Diego.
- Honarpour, M., Koederitz, L. and Harvey, A.H. 1986, *Relative Permeability of Petroleum Reservoirs*, CRC Press, Boca Raton, Florida, 43 pp.
- <http://info.ngwa.org/gwol/pdf/911552617.PDF>
- http://www.accessengineeringlibrary.com/mghpdf/007162113X_ar021.pdf
- <http://www.airwaysmuseum.com/Radar%20in%20ATC%20paper%20c70s.htm>
- <http://www.archaeophysics.com/burials/index.html>
- <http://www.earthdyn.com/geophysical/GPR/GPR.html>
- http://www.ehow.com/list_6158395_types-ground-penetrating-radar.html
- <http://www.geophysical.com>
- <http://www.innovateus.net/science/what-are-different-uses-radar>
- <http://www.malags.com>
- <http://www.sensoft.ca>
- <http://www.sensoft.ca/Applications/Mining-Tunneling-and-Quarrying.aspx>
- Huling, S.G., and J.W. Weaver, 1991. Dense nonaqueous phase liquids, *Ground Water Issue*, EPA/540/4-91-002, U.S.EPA, R.S. Kerr Environ. Res. Lab., Ada, OK, 21 pp.
- I.M. Cozzarelli, B.A. Bekins, M.J. Baedecker, G.R. Aiken, R.P. Eganhouse and M.E. Tuccillo, Progression of natural attenuation processes at a crude-oil spill site: I. Geochemical evolution of the plume, *Journal of Contaminant Hydrology* 53 (2001), pp. 369–385.
- I.M. Cozzarelli, M.J. Baedecker, R.P. Eganhouse and D.F. Goerlitz, The geochemical evolution of low-molecular-weight organic acids derived from the degradation of petroleum

contaminants in groundwater, *Geochimica et Cosmochimica Acta* 58 (1994), pp. 863–877.

I.M. Cozzarelli, M.J. Baedecker, R.P. Eganhouse and D.F. Goerlitz, The geochemical evolution of low-molecular-weight organic acids derived from the degradation of petroleum contaminants in groundwater, *Geochimica et Cosmochimica Acta* 58 (1994), pp. 863–877.

J.H. Bradford, GPR offset dependent reflectivity analysis for the characterisation of a high conductivity LNAPL plume, *Proceedings of the Symposium on the Application of Geophysics to Engineering and Environmental Problems (SAGEEP)* (2003), pp. 238–252.

J.J. Daniels, R. Roberts and M. Vendl, Ground penetrating radar for the detection of liquid contaminants, *Journal of Applied Geophysics* 33 (1995), pp. 195–207.

J.M. Carcione and G. Seriani, An electromagnetic modelling tool for the detection of hydrocarbons in the subsoil, *Geophysical Prospecting* 48(2) (2000), pp. 231–256.

J.M. Carcione, D. Gei, M. Botelho, A. Osella and M. del la Vega, Fresnel reflection coefficients for GPR-AVA analysis and detection of seawater and NAPL contaminants, *Near Surface Geophysics* 4 (4) (2006), pp. 253–263.

J.M. Carcione, G. Seriani and D. Gei, Acoustic and electromagnetic properties of soils saturated with salt water and NAPL, *Journal of Applied Geophysics* 52 (2003), pp. 177–191.

J.M. Carcione, H. Marcak, G. Seriani and G. Padoan, GPR modeling study in a contaminated area of Krzywa Air Base (Poland), *Geophysics* 65 (2) (2000), pp. 521–525.

Jutta Hager, Mario Carnevale, Brian R. Jones, Unconventional deep-water investigation of drilling obstructions. (USA, MA). pp.757-764

J.M. Reynolds, *An Introduction to Applied and Environmental Geophysics* (1997).

K.W. Sneedon, G.R. Olhoeft and M.H. Powers, Determining and Mapping DNAPL Saturation Values From Non-Invasive GPR Measurements, *Proceedings of the Symposium on the Application of Geophysics to Engineering and Environmental Problems (SAGEEP)* (2000), pp. 293–301.

Kessler, A. and Rubin, H. 1987, Relationship between water infiltration and oil spill migration in sandy soils, *Journal of Hydrology*, 91: 187-204.

Knoll MD. 1996. A petrophysical basis for ground penetrating radar and very earlytime electromagnetics: electrical properties of sand-clay mixtures. PhD thesis. Univ. BC, Vancouver, Can. 316 pp.

Kueper, B.H. and Frind, E.O. 1991b, Two-phase flow in heterogeneous porous media: Model application, *Water Resources Research*, 27(6): 1059-1070.

Kueper, B.H. and Gerhard, J.I. 1995, Variability of point source infiltration rates for two-phase flow in heterogeneous porous media, *Water Resources Research*, 31(12): 2971-2980.

Lucius JE, Olhoeft GR, Hill PL, Duke SK. 1992. Properties and Hazards of 108 Selected

Substances. US Geol. Surv. Open File Rep., 92- 527. USGS, Denver, Colo.

Lucius, S. E., Olhoeft, G. R., Hill, P. L., and Duke, S. K., 1990, Properties and hazards of 108 selected substances: U. S. Geological Survey Open File Report 90-408, 559 p.

M.J. Baedecker and I.M. Cozzarelli, Biogeochemical processes and migration of aqueous constituents in ground water contaminated with crude oil. In: A.R. Dutton, Editor, Toxic Substances and the Hydrologic Sciences, American Institute of Hydrology, Austin, TX (1994), pp. 69–79.

Mario Carnevale, Jutta Hager and Brian R. Jones. 2005. Integrated geophysical characterization at a contaminated site.

Mercer, J.W. and Cohen, R.M. 1990, A review of immiscible fluids in the subsurface: Properties, models, characterization and remediation, Journal of Contaminant Hydrology, 6: 107-163.

Miller, C.T., Christakos, G., Imhoff, P.T., Mc Bride, J.F., Pedit, J.A., Pedit and Trangenstein, J.A. 1998, Multiphase flow and transport modeling in heterogeneous porous media: challenges and approaches, Advances in Water Resources, 21(2): 77-120.

N.J. Cassidy, Dielectric Properties of Free-Phase Hydrocarbon Contamination: Implications for GPR investigation, IEEE Proceedings of the 10th International Conference on Ground-Penetrating Radar GPR2004, Netherlands (2004), pp. 551–554.

N.J. Cassidy, Evaluating LNAPL contamination using GPR signal attenuation analysis and dielectric property measurements: Practical implications for hydrological studies, Journal of Contaminant Hydrology 94 (2007) 49– 7 (2006).

N.J. Cassidy, GPR Signal Dispersion and Attenuation Characteristics of LNAPL Hydrocarbon Contamination, IEEE Proceedings of the 11th International Conference on Ground Penetrating Radar, GPR2006, Ohio, USA (2006), pp. 1–8.

O. Mazác, L. Benes, I. Landa and A. Maskova, Determination of the extent of oil contamination in ground water by geoelectrical methods. In: S.H. Ward, Editor, Geotechnical and Environmental Geophysics vol. II, Society of Exploration Geophysicists (1990), pp. 107–112.

Olhoeft GR. 1998. Electrical, magnetic and geometric properties that determine ground penetrating radar performance. Int. Conf. Ground Penetrating Radar, 7th, Lawrence, pp. 177–82. Univ. Kansas.

Olhoeft, 1992 G.R. Olhoeft, Geophysical detection of hydrocarbon and organic chemical contamination. In: R.S. Bell, Editor, Proceedings on Application of Geophysics to Engineering, and Environmental Problems, Society of Engineering and Mining Exploration Geophysics, Golden, CO, Oakbrook, IL (1992), pp. 587–595.

Olhoeft, G. R. and King, T. V. V., 1991, Mapping subsurface organic compounds noninvasively by their reactions with clays: U. S. Geological Survey Toxic Substances Hydrology Program - Proc. of the technical meeting, Monterey, CA, March 11-15, 1991, U. S.

Geological Survey Water Resources Investigations Report 91-4034, p. 552-557.

P.B. McMahon, D.A. Vrobleskey, P.M. Bradley, F.H. Chapelle and C.D. Gullet, Evidence for enhanced mineral dissolution in organic-rich shallow ground water, *Ground Water* 33 (1995), pp. 207–216.

P.M. Barone, A. Di Matteo, F. Graziano, E. Mattei, E. Pettinelli, GPR application to the structural control of historical buildings: two case studies in Rome, Italy (2010).

P.M. Baronei, F.Graziano,E.Pettinelli and R.Ginannicorradini. Ground-penetrating Radar Investigations into the Construction Techniques of the Concordia Temple (Agrigento,Sicily,Italy).

Plumb, R. H. and Pitchford, A. M., 1985, Volatile organic scans--Implications for ground water monitoring: Proc. of the API and NWWA Conf. on Petroleum Hydrocarbons and Organic Chemicals in Ground Water - Prevention, Detection, and Restoration, Nov. 13-15, 1985, Houston, TX, p. 207-222.

Poulsen, M.M. and Kueper, B.H. 1992, A field experiment to study the behaviour of tetrachloroethylene in unsaturated porous media, *Environmental Science and Technology*, 26(5): 889-895

Powers M. 1997. Modeling frequency dependent GPR. *Lead. Edge.* 16:1657–62.

R. Joyce, C. Vukenkeng, E. Atekwana, D. Werkema, S. Rossbach, G. Abdel Aal, C. Davis and J. Nolan. 2008. Temporal geophysical investigations of the FT-2- plume at the Wurtsmith Air Force Base, Oscoda, Michigan.

R.I. Acworth, Physical and chemical properties of a DNAPL contaminated zone in a sand aquifer, *Quarterly Journal of Engineering Geology and Hydrology*34 (2001), pp. 85–98.

Sander KA. 1994. Characterization of DNAPL movement in saturated porous media using ground penetrating radar. MS thesis. Colo. Sch. Mines, Golden. 258 pp.

Schowalter, T.T. 1979, Mechanics of secondary hydrocarbon migration and entrapment, *Am. Assoc.Pet. Geol. Bull.*, 63(5): 723-760.

Van der Roest, P.B., Brassler, DJ S., Wagebaerst, A.PJ, and Stam, P.H. 1997. Zeroing in on hydrocarbons. *Environ. Prot.*, 8, 5, 44-46.

Van Geel, P.J. and Sykes, J.F. 1997, The importance of fluid entrapment, saturation hysteresis and residual saturations on the distribution of a lighter-than-water non-aqueous phase liquid in a variably saturated sand medium, *Journal of Contaminant Hydrology*, 25: 249-270.

W.A. Sauck, E.A. Atekwana and M.S. Nash, High conductivities associated with an LNAPL plume imaged by integrated geophysical techniques, *Journal of Environmental and Engineering Geophysics* 2–3 (1998), pp. 203–212.

Ward SH, Hohmann GW. 1988. Electromagnetic theory for geophysical applications. In *Electromagnetic Methods in Applied Geophysics*, ed. MN Nabighian, 1:130–311. Tulsa, OK:

Soc. Explor. Geophys.

Yong Keun Hwang, Anthony L. Endres, Scott D. Piggott and Beth L. Parker. 2006. GPR monitoring of a DNAPL release in a natural groundwater flow field.